



Spring 2002

# Paleogeography of the Spieden Group, San Juan Islands, Washington

Patricia Allison Dean  
*Western Washington University*

Follow this and additional works at: <https://cedar.wwu.edu/wwuet>



Part of the [Geology Commons](#)

---

## Recommended Citation

Dean, Patricia Allison, "Paleogeography of the Spieden Group, San Juan Islands, Washington" (2002). *WWU Graduate School Collection*. 823.  
<https://cedar.wwu.edu/wwuet/823>

This Masters Thesis is brought to you for free and open access by the WWU Graduate and Undergraduate Scholarship at Western CEDAR. It has been accepted for inclusion in WWU Graduate School Collection by an authorized administrator of Western CEDAR. For more information, please contact [westerncedar@wwu.edu](mailto:westerncedar@wwu.edu).

PALEOGEOGRAPHY OF THE SPIEDEN GROUP,  
SAN JUAN ISLANDS, WASHINGTON

---

BY

Patricia Allison Dean

Accepted in Partial Completion  
of the Requirements for the Degree  
Master of Science  
Geology

---

Moheb A. Ghali, Dean of Graduate School

ADVISORY COMMITTEE

---

Chair, Dr. Bernie Housen

---

Dr. Chris Suezek

---

Dr. Susan DeBari

---

Dr. Russell Burmester

## MASTERS THESIS

In presenting this thesis in partial fulfillment of the requirements for a master's degree at Western Washington University, I agree that the Library shall make its copies freely available for inspection. I further agree that extensive copying of this thesis is allowable only for scholarly purposes. It is understood, however, that any copying or publication of this thesis for commercial purposes, or for financial gain, shall not be allowed without my written permission.

Signature \_\_\_\_\_

Date May 24, 2002

## MASTER'S THESIS

In presenting this thesis in partial fulfillment of the requirements for a master's degree at Western Washington University, I grant to Western Washington University the non-exclusive royalty-free right to archive, reproduce, distribute, and display the thesis in any and all forms, including electronic format, via any digital library mechanisms maintained by WWU.

I represent and warrant this is my original work and does not infringe or violate any rights of others. I warrant that I have obtained written permissions from the owner of any third party copyrighted material included in these files.

I acknowledge that I retain ownership rights to the copyright of this work, including but not limited to the right to use all or part of this work in future works, such as articles or books.

Library users are granted permission for individual, research and non-commercial reproduction of this work for educational purposes only. Any further digital posting of this document requires specific permission from the author.

Any copying or publication of this thesis for commercial purposes, or for financial gain, is not allowed without my written permission.

Name: Patricia Dean

Signature: \_\_\_\_\_

Date: May 22, 2018

PALEOGEOGRAPHY OF THE SPIEDEN GROUP,  
SAN JUAN ISLANDS, WASHINGTON

---

A Thesis

Presented to the Faculty of  
Western Washington University

---

In Partial Fulfillment  
of the Requirements for the Degree  
Master of Science

---

BY

Patricia Allison Dean

June 2002

## ABSTRACT

The Spieden Group in the San Juan Islands of Washington State consists of the Lower Cretaceous Sentinel Island Formation and the Upper Jurassic Spieden Bluff Formation. In order to constrain the location of its origin, paleomagnetism of the sedimentary rocks of the Spieden Group was studied to obtain paleolatitudes. Two components of magnetization were measured in most of the Sentinel Island Formation specimens. The second-removed component had a mean in-situ direction of  $D = 34.1^\circ$ ,  $I = 44.2^\circ$ ,  $\alpha_{95} = 12.0^\circ$  and a mean tilt-corrected direction of  $D = 49.3^\circ$ ,  $I = 71.5^\circ$ ,  $\alpha_{95} = 6.9^\circ$ . Uncertainty that some of the scatter of directions was due to fault block rotation not corrected for during unfolding suggests inclination-only analysis may be appropriate; it yielded a tilt-corrected inclination of  $I = 64.0^\circ$ ,  $\alpha_{95} = 7.9^\circ$ . Three components of magnetization were extracted from most of the Spieden Bluff Formation specimens. The third-removed component had a mean in-situ direction of  $D = 82.5^\circ$ ,  $I = 82.0^\circ$ ,  $\alpha_{95} = 23.0^\circ$  and a mean tilt-corrected direction of  $D = 78.3^\circ$ ,  $I = 71.3^\circ$ ,  $\alpha_{95} = 16.9^\circ$ . Segregating directions according to how much a component contributed to the total remanence isolated characteristic components that were unfolded incrementally. The best clustered direction was from components that constituted 70-80% of NRM intensity and yielded a magnetic direction of  $D = 48.2^\circ$ ,  $I = 65.0^\circ$ ,  $\alpha_{95} = 20.9^\circ$ . The Cretaceous still-stand pole was used as a reference pole for the Cretaceous Sentinel Island Formation. The expected paleomagnetic direction calculated for the present position of the Sentinel Island Formation of  $D = 334.6^\circ$ ,  $I = 74.0^\circ$  corresponds to a latitude of  $60^\circ$  N. This latitude

contrasts with the paleolatitude best estimate of origin for the Sentinel Island Formation (derived from its  $64^\circ$  inclination) of  $45.7^\circ$  N latitude. The pole of the Brushy Basin Member of the Morrison Formation was used as a reference pole for the Jurassic Spieden Bluff Formation. The expected paleomagnetic direction calculated for the Jurassic Spieden Bluff Formation of  $D = 327.4^\circ$ ,  $I = 65.3^\circ$  corresponds to a latitude of  $47^\circ$  N, which is identical to the paleolatitude for the Spieden Bluff Formation derived from its  $65^\circ$  inclination.

## ACKNOWLEDGEMENTS

Thanks to Bernie Housen, Russ Burmester, Chris Suczek, Sue DeBari, Dave Engebretson and Myrl Beck for their help in performing fieldwork and in writing.

Thanks to George Mustoe, Chris Sutton, Vicki Critchlow and Mike McMullen for their help and support. Thanks to Phyllis Gregoire, Tammy Fawcett, Elizabeth Kilanowski, Andy Knowles, Chad Hults, Zan Frederick, and the practical paleomag class for helping collect samples.

Thanks to Jim Haggart of the Geological Survey of Canada for identification of fossils found in the Sentinel Island Formation.

Thanks to the owner of Spieden Island for allowing us access to its beautiful outcrops and to the Nature Conservancy for allowing access to Sentinel Island.

Thanks to Chad McCabe for his program CryoThing used in the measurement of specimens.

And thanks for funding of this project by Western Washington University Geology Department and Graduate School, the Geological Society of America and the Pacific Northwest Paleomagnetism Laboratory. Funds for the Pacific Northwest Paleomagnetism Laboratory include National Science Foundation (NSF) grants EAR-9727032 (Superconducting Magnetometer), and EAR-9726884 (AF and thermal demagnetizers). Other support for this project was provided by NSF grants OCE-9796173 and EAR-0073888.



## Table of Contents

List of Tables	p. viii
List of Figures	p. ix
1. Introduction	p. 1
2. Geology	p. 3
3. Geochronology	p. 5
4. Paleomagnetism	p. 6
4.1 Methods	p. 6
4.2 Results for the Cretaceous Sentinel Island Formation	p. 9
4.3 Results for the Jurassic Spieden Bluff Formation	p. 9
5. Rock Magnetism	p. 10
6. Magnetic Fabrics	p. 11
7. Analysis	p. 12
7.1 Age of Magnetism	p. 12
7.2 Inclination Error	p. 13
8. Discussion – Tectonic Implications	p. 14
9. Conclusion	p. 17
10. References Cited	p. 19
Tables	p. 23
Figures	p. 30

## List of Tables

- Table 1. Fossil and fossil assemblages of the Lower Cretaceous Sentinel Island Formation.
- Table 2. Site-averaged in-situ paleomagnetic data of the first-removed component for the Sentinel Island Formation.
- Table 3. Site-averaged in-situ paleomagnetic data of the second-removed component for the Sentinel Island Formation.
- Table 4. Inclination-only data - Incremental unfolding of paleomagnetic data using intensity-selected characteristic components for the Sentinel Island Formation.
- Table 5. Incremental unfolding of paleomagnetic data using intensity-selected characteristic components for the Sentinel Island Formation.
- Table 6. Site-averaged in-situ paleomagnetic data of the first-removed component for the Spieden Bluff Formation.
- Table 7. Site-averaged in-situ paleomagnetic data of the second-removed component for the Spieden Bluff Formation.
- Table 8. Site-averaged in-situ paleomagnetic data of the third-removed component for the Spieden Bluff Formation.
- Table 9. Incremental unfolding of paleomagnetic data using intensity-selected characteristic components for the Spieden Bluff Formation.

## List of Figures

- Figure 1 Location map of the San Juan Islands.
- Figure 2 Location map for the faults and geographic names in the San Juan Islands.
- Figure 3 Location of paleomagnetic sites and geology of the Spieden Group.
- Figure 4 Stratigraphy of the Spieden Group.
- Figure 5 Cross-section showing general structures and inferred block movement within the Spieden Group.
- Figure 6 Equal area plots showing bedding planes for (a) Jurassic Spieden Bluff Formation and (b) Cretaceous Sentinel Island Formation.
- Figure 7 Sentinel Island Formation demagnetization diagrams.
- Figure 8 Equal area plots of characteristic directions for the Sentinel Island Formation.
- Figure 9 Fold test of the Sentinel Island Formation directions.
- Figure 10 Representative demagnetization diagrams of the Spieden Bluff Formation.
- Figure 11 Equal area plots of site-mean directions of (a) first-removed and (b) second-removed components for the Spieden Bluff Formation.
- Figure 12 Equal area plots of characteristic directions of the Spieden Bluff Formation.
- Figure 13 Fold test of the Spieden Bluff Formation directions.
- Figure 14 Magnetic susceptibility verses temperature experiments.
- Figure 15 Low temperature susceptibility experiments.
- Figure 16 Representative hysteresis loops for the Sentinel Island and Spieden Bluff formations.
- Figure 17 Day et al. (1977) plots for the hysteresis data for the Spieden Group.

- Figure 18 Anisotropy of magnetic susceptibility (AMS) and bedding directions for the (a) Sentinel Island and (b) Spieden Bluff formations.
- Figure 19 Flinn diagrams of AMS data for the Sentinel Island and Spieden Bluff formations.
- Figure 20 Incremental fold tests for the Cretaceous Sentinel Island Formation directions.
- Figure 21 Fold tests of site 6 of the Spieden Bluff Formation.
- Figure 22 Equal area diagrams showing site level directions for the Spieden Bluff Formation.
- Figure 23 Magnetic anisotropy (AMS), plotted as  $1/P$  (degree of anisotropy) verses tangent of inclination for the Sentinel Island and Spieden Bluff formations.
- Figure 24 Reconstruction maps for the paleolatitudes of the Spieden Group.

## 1. INTRODUCTION

The San Juan Islands of northwest Washington State (Fig. 1) are composed of terranes ranging in age from Paleozoic to Cretaceous (Brandon et al., 1988). Most of these terranes underwent tectonic burial of up to 20 km, then uplift by 85 Ma (Brandon et al., 1988). A first order problem is to determine the origin of these terranes with respect to each other and to their present location on the North American margin. The Spieden Group, part of the Haro terrane in the San Juan Islands, is made up of rocks characteristic of shallow marine, volcanic-arc and alluvial fan settings (Johnson, 1981) (Fig. 2). One constraint on the location of origin of the Spieden Group is paleolatitude, which can be determined qualitatively by using climate-diagnostic fossils or quantitatively using paleomagnetism.

The Spieden Group is located within the San Juan thrust system. The terranes within this thrust system are fault-bounded blocks with different geological histories. The rocks of the San Juan thrust system can be divided into two components on the basis of their metamorphic histories. The internal units (Fig. 2) are mostly exposed in the southern islands and include rock units that have been subjected to high pressure, low temperature metamorphism (Brandon et al., 1988). Thrusting of these rocks occurred middle to late in the Cretaceous (Misch, 1966, Whetten et al., 1978, 1980). Prior paleomagnetic studies on the internal units have found that the vast majority of the rocks are remagnetized, most likely during Late Cretaceous deformation or metamorphism and have been rotated, translated or tilted considerably since then (Bogue et al., 1989 and Burmester et al., 2000). Rocks of the external units escaped the high-pressure metamorphism of the internal units but were folded either in the Cretaceous (Brandon et al., 1988) or during a

younger (Eocene age) deformational event known as the Cowichan fold and thrust event (England and Calon, 1991). The external units are made up of the Haro Terrane (consisting of the Upper Triassic Haro Formation and the Jura-Cretaceous Spieden Group) and the Upper Cretaceous syn-orogenic Nanaimo Group (Brandon et al., 1988). The Spieden Group lies between the Haro Formation to the south and the Nanaimo Group to the north (Fig. 2). Sub-marine faults are assumed to separate these formations. Although a pilot study of the Haro Formation indicates it is remagnetized (Hults and Housen, 2000), paleomagnetic results indicate that the Nanaimo Group is not remagnetized (Ward et al., 1997; Housen et al. 1998; Enkin et al., 2001). The age, location within the external units, and lack of metamorphism make the Spieden Group a good target for a paleomagnetic study.

Many of the terranes located outboard of the North American craton have been translated by interaction between offshore oceanic plates and North America (e.g., Beck, 1976). Plate tectonic reconstructions by Engebretson et al. (1985) indicate that sinistral relative motion between North American and oceanic plates along the North American margin probably occurred prior to the mid-Cretaceous. This plate interaction could have displaced coastal terranes as much as 3000 km to the south (Irving 1979; Beck, 1989). Tectonic reconstructions for the mid-Cretaceous suggest a shift to dextral relative motion between North America and adjacent oceanic plates, which moved many of the outboard terranes northward by several 1000 km (Engebretson et al., 1985). May and Butler (1989) termed this left-lateral to right-lateral motion the “yo-yo” effect. Monger et al. (1994), using geological evidence, suggested that sinistral displacement along the North American margin took place after the Early Jurassic and dextral displacement after the



mid-Cretaceous. Although there is no consensus that all Jurassic and Cretaceous rocks have been translated, one key to documenting the amount and timing of such translation along the margin is to determine the paleolatitudes of Upper Jurassic and Lower Cretaceous sedimentary rocks that occur in many of these terranes. Brandon et al. (1988) suggested that the Lower Jurassic to Upper Cretaceous clastic sedimentary units in the San Juan Island and North Cascade systems (Nooksack, Lummi, Constitution, Spieden and Kyuquot groups) comprise an overlap sequence that links these terranes to the North American continent. McClelland et al. (1992) extended this argument to include nearly all Upper Jurassic and Lower Cretaceous clastic marine sediments that filled small basins along the entire inboard margin of the Alexander-Wrangellia-Peninsular amalgamated terrane.

Johnson (1981) concluded that there is no local source for the types of volcanic clasts found in the Spieden Group, indicating a far removed source or origin. Paleomagnetic results can aid in constraining the source of these sediments by determining the latitude at which they accumulated. The paleolatitude determined provides insight to the location of the Spieden Group's origin and helps constrain the timing of its accretion and the latitude at which the Spieden Group and the San Juan Island System docked to North America.

## **2. GEOLOGY**

The Spieden Group consists of two formations, the Upper Jurassic Spieden Bluff Formation and the Lower Cretaceous Sentinel Island Formation (Fig. 3). The Spieden Bluff Formation has an exposed thickness of approximately 100 meters and contains volcanic breccia and conglomerate, sandstone, siltstone and tuff (Johnson, 1981) (Fig. 4).

The base of this formation is not exposed. The lower member consists of 5 m of fine-grained lithic arenite and tuff overlain by 75 m of volcanic breccia and conglomerate. The upper member consists of 20 m of fine- to medium-grained sandstone and siltstone (Johnson, 1981). The Spieden Bluff Formation is overlain by the Lower Cretaceous Sentinel Island Formation on an angular unconformity (Johnson, 1981). The Sentinel Island Formation is 740 meters thick and is composed of volcanic conglomerate, sandstone and siltstone (Johnson, 1981) (Fig. 4). The lower member is composed of massive sandstone and siltstone. The upper member is made up of a conglomerate containing igneous clasts. Bedding thickness ranges from 5 cm to 5 m.

The structures of the two formations, as mapped by Johnson (1981), differ in their folding style (Fig. 5). The Upper Jurassic Spieden Bluff Formation contains large sinusoidal folds (Johnson, 1981). These folds are exposed in the eastern outcrops of the formation and have amplitudes of 5 m and wavelengths of up to 15 m (Johnson, 1981). Slump folds are also prevalent in some of the siltstone layers. Most of the Spieden Bluff Formation is only gently folded. The Sentinel Island Formation is tilted steeply towards the southwest. Folding is not prevalent at the outcrop scale in the Sentinel Island Formation, although the bedding dips change from  $80^\circ$  in the north to  $30^\circ$  in the south (Fig. 3).

Fold axes for the Sentinel Island Formation, as determined by girdles to bedding-plane poles, are sub-horizontal, with a trend of  $290^\circ$  (Fig. 6a). Fold axes for the Spieden Bluff Formation are also sub-horizontal, with a trend of  $280^\circ$  (Fig. 6b).



Johnson (1981) noted many small faults with indeterminate amounts of displacement on the outcrop scale. Local vertical-axis rotations may have occurred between blocks separated by these faults, as well as between large slump blocks.

### 3. GEOCHRONOLOGY

The age of the upper member of the Spieden Bluff Formation has been determined to be Late Jurassic or younger (152 +/- 4 Ma) by K-Ar dating of hornblende from an angular clast of fresh andesite (Tabor cited by Johnson, 1981). This upper member was also determined to be Late Jurassic (Oxfordian or Kimmeridgian) by the occurrence of *Buchia concentrica* (McLellan, 1927), an indicator of this time interval.

The Sentinel Island Formation was determined to be Lower Cretaceous by the presence of diagnostic fossils and isotopic methods. Early Cretaceous fossils of *Buchia crassicollis solida* with an age of uppermost Valanginian (138 to 131 Ma) were found in the lower member of the Sentinel Island Formation (McLellan, 1927, Haggart, 2000). Three clasts in the upper member were dated using K-Ar (Johnson, 1981). A dacite porphyry clast collected by R. W. Tabor was determined to be 145 +/- 3 Ma (Johnson, 1981). A second dacite porphyry clast yielded a zircon fission track age of 138 +/- 16 and an apatite fission track age of 147 +/- 22 Ma (Johnson, 1981; Brandon et al., 1988). A zircon obtained from a granodiorite clast yielded a fission track age of 147 +/- 20 Ma (Johnson, 1981).

The radiometric ages of the volcanic clasts and the fossils in the sedimentary rocks provide upper- and lower-most age constraints respectively. The volcanic clasts and tuff bed indicate a nearby volcanic source for the Spieden Group.

Jim Haggart of the Geological Society of Canada examined fossils and fossil assemblages of the thicker beds of the Lower Cretaceous Sentinel Island Formation (site 19) (Fig. 3) collected during this investigation (Table 1). The presence of framework-supported buchiid shells indicates that the Sentinel Island Formation was deposited in a shallow marine environment during the Late Valanginian (Haggart, 2000). These fossil assemblages were found to be dominated by taxa typically found in high (45° and higher) latitudes.

## **4. PALEOMAGNETISM**

### **4.1 Methods**

Methods of sample collection, preparation, laboratory measurement and analysis followed standard paleomagnetic procedures (Tauxe, 1998). Oriented paleomagnetic cores were acquired in the field by drilling using portable coring equipment. 141 cores from 9 sites were collected from the upper portion of the Spieden Bluff Formation, 49 cores from 6 sites from the lower portion of the Sentinel Island Formation, and 28 cores from 4 sites in the upper portion of the Sentinel Island Formation. The outcrops sampled in the Spieden Bluff Formation are shoreline exposures of well-bedded, fine-grained mudstones, limestones and tuffs. Outcrops sampled in the Sentinel Island Formation have clear and predominant bedding and are fine to coarse grained, volcanic-lithic sandstones along with fine-grained mudstones. When possible, core azimuths were measured with both sun and magnetic compass to allow for correction of local magnetic anomalies. Each core was cut into 10-cc specimens that were designated with labels “a” to “c” (top to bottom of core). Measurements were then performed on specimen c or b if possible to decrease the effects of weathering. Natural remanent magnetization (NRM)

for 131 specimens from 218 cores was measured on a 2G Enterprises DC SQUID rock magnetometer (model 755). Of these, 13 were subjected to pilot alternating field (AF) demagnetization in steps of either 2.5 or 5 mT from 2.5 to 100 mT using a D-Tech D-2000 demagnetizer. Demagnetization paths were not simple, so the remaining 118 specimens were progressively thermally demagnetized in increments of 50°C from 0 to 300°C, 20°C from 300 to 500°C and 10°C from 500 to 580°C in an ASC TD-48 thermal demagnetizer. All the instruments were located within a Lodestar Magnetics magnetically shielded room with an ambient field around 350 nT. Demagnetization results were visually inspected using orthogonal diagrams (Zijderveld, 1967). Directions of linear segments were determined with principal component analysis (PCA) (Kirschvink, 1980). The maximum angular deviation (MAD) calculated for the PCA line fits provides a good criterion for determining how well the demagnetization data define a linear path. Large MAD values indicate that a linear fit is poorly defined. For this study, line fits with MAD values greater than twenty degrees were rejected from further analysis. Site-mean directions and statistics were calculated using the method of Fisher (1953). A few directions that passed the MAD screening were later rejected as outliers according to the method of van Damme (1994).

To avoid prejudicing interpretation by assuming a relationship between stability of remanence to demagnetization and its stability over the rock's history, two methods of categorizing directions were employed. The first method separated line segments into first-, second- and (where present) third-removed components regardless of the absolute or relative lengths of each straight line segment. Components selected this way will be referred to as first-, second- or third-removed components. The second method identifies

the characteristic components by how much of their original intensity (NRM) was represented by straight-line segments. Component segments were analytically determined by dividing the difference of intensities at the beginning and end of the segments of each component removed by the total intensity. Grouping of these characteristic components was based on whether the straight-line segments represented 60-70%, 70-80% or 80-90% of the NRM intensity. These groupings of intensity-based characteristic components are referred to as ChRM60, ChRM70 and ChRM80 respectively.

Fold-tests using McElhinney (1964) and Tauxe and Watson (1994) methods were performed to constrain the age of magnetization relative to folding. McElhinney's method compares the Fisher (1953) precision parameter  $k$  calculated in in-situ coordinates with  $k$  calculated in tilt-corrected coordinates. If  $k$  is significantly higher in tilt-corrected coordinates, the magnetization direction passes the fold test, which means the age of the remanence pre-dates folding. The Tauxe and Watson (1994) fold-test method uses a bootstrap method to evaluate the relationship between bedding attitude and clustering of remanence directions. Their parameter,  $\tau$ , is analogous to  $k$  in that  $\tau$  increases as the clustering of directions is improved. For both types of tests, site mean directions were used.

Vertical axis rotation of fault blocks or slump folds (see structure section) may have caused scatter of declinations. Averaging such scattered directions will bias the mean inclination to values that are too steep. To get around this, a method of calculating the mean inclination from inclination-only data (Briden and Ward, 1962; McFadden and Reid, 1982) was also used. The fold test using this method is similar to the above fold tests in that the directions were incrementally corrected to paleohorizontal, but differed in



that only the inclinations at each correction were used with the inclination-only method to calculate a mean inclination and statistics.

#### 4.2 Results for Cretaceous Sentinel Island Formation

Orthogonal demagnetization diagrams for thermal demagnetization of specimens from the Cretaceous Sentinel Island Formation (Fig. 7) show either one or two remanence components. In specimens with two components, the first-removed component unblocks at  $\sim 300^{\circ}\text{C}$ . The second-removed component has an unblocking temperature between  $\sim 500^{\circ}$  and  $580^{\circ}\text{C}$ . Out of the nine sites collected, two (sites 11 and 12) were dropped from the study because the majority of the samples disintegrated during the preparation process. Out of the eight sites remaining, five (13, 14, 17, 19, 20) had circles of 95% confidence ( $\alpha_{95}$ )  $< 14^{\circ}$  for the second-removed component. The in-situ mean directions for the first- and second-removed components are listed in Tables 2 and 3. Comparisons of in-situ with tilt-corrected directions are shown in Figure 8.

Inclinations of characteristic components based on ratios of intensity were unfolded in 10-degree steps (Table 4). Figure 9 shows unfolding of characteristic components of the Sentinel Island Formation for ChRM60, ChRM70 and ChRM80 (Table 5).

#### 4.3 Results for Jurassic Spieden Bluff Formation

Thermal demagnetization of specimens from the Jurassic Spieden Bluff Formation reveals that the remanence consists of either two or three components. In three-component specimens, the unblocking temperature ranges for the first-, second- and third-removed components are  $\sim 0$  to  $200^{\circ}\text{C}$ ,  $\sim 200$  to  $400^{\circ}\text{C}$  and  $\sim 400$  to  $580^{\circ}\text{C}$ ,

respectively. Representative demagnetization plots (Zijderveld, 1967) for the Upper Jurassic Spieden Bluff Formation are presented in Figure 10.

Out of the nine sites collected, two (2 and 5) were dropped from the study because they have fewer than three specimens with stable demagnetization behavior. The seven sites remaining yield mean in-situ first-, second- and third-removed components (MAD less than 20). These components are listed in Tables 6, 7 and 8. Figure 11 is an equal area projection of the first- and second-removed components.

Third component directions calculated for the Jurassic Spieden Bluff Formation are scattered. The tilt-corrected mean direction calculated from the third component is listed in Table 8. Comparisons of in-situ with tilt-corrected mean directions are shown in Figure 12. Figure 13 shows unfolding of characteristic components using the Tauxe and Watson (1994) fold test in incremental unfolding steps of ChRM60, ChRM70 and ChRM80 intensity (Table 9).

## **5. ROCK MAGNETISM**

Curie temperatures were estimated using a KLY-3S Kappabridge unit with a high temperature furnace and an argon atmosphere. A low temperature cryostat was employed to determine the contribution of paramagnetic minerals to susceptibility. Hysteresis measurements were made with a Princeton Measurements model 2900 VSM at the Institute for Rock Magnetism at the University of Minnesota.

Susceptibility versus temperature curves have pronounced drops in susceptibility between 560° and 580 °C, corresponding to the Curie temperature of magnetite (Fig. 14). For diamagnetic minerals such as quartz, calcite and feldspar, susceptibility is constant. Susceptibility as a function of temperature for paramagnetic minerals such as iron-

bearing mica, amphiboles, clays and ferromagnetic minerals above their Curie temperatures follows the Curie-Weiss law (Dunlop and Ozdemir, 1997),  $k = C [1/(T - \theta)]$ , where  $k$  is the measured susceptibility,  $C$  is the intrinsic susceptibility,  $T$  is the temperature in Kelvin and  $\theta$  is the paramagnetic Curie temperature. Low temperature susceptibility measurements (Fig. 15) indicate (with a few exceptions) that paramagnetic minerals dominate the susceptibility of these samples. In some samples an increase in susceptibility at 120 K is interpreted as the Verwey transition in magnetite. In these samples, magnetite likely dominates the bulk susceptibility and perhaps anisotropy of magnetic susceptibility (AMS) as well.

Magnetic hysteresis was measured to check for unusual hysteresis properties that might indicate remagnetization (Channell and McCabe, 1994). No unusual (i.e., wasp-waisted) loops were measured in either the Sentinel Island or Spieden Bluff formations (Fig. 16). Day et al. (1977) plots show the trend expected for a mixture of pseudo-single-domain (PSD) and multi-domain (MD) magnetite (Fig. 17).

## 6. MAGNETIC FABRICS

Anisotropy of magnetic susceptibility was determined using a KLY-3S Kappabridge. Consistent directions of maximum susceptibility might be produced by paleocurrents or intersection of bedding with an incipient cleavage formed during folding or faulting, and degree of anisotropy should correlate with inclination if inclination-flattening was a factor in paleomagnetic directions.

Anisotropy of magnetic susceptibility (AMS) shows very good correspondence between the bedding and the susceptibility ellipsoids (Fig. 18). Some sites (Ksi-14, for example) have AMS fabrics that are slightly imbricated relative to bedding (Fig. 18a).

This imbrication is most likely related to paleocurrents. Johnson (1981) determined paleocurrent indicators and imbrication in both the formations. Preferred orientation of clasts in the Spieden Bluff Formation show direction of north to south transport and northeast to southwest transport in the thinner beds of the Sentinel Island Formation. Flinn diagrams shown in Figure 19 indicate that AMS fabrics predominately are oblate (flattened).

## 7. ANALYSIS

### 7.1 Age of Magnetism

One hypothesis is that magnetization in these rocks was acquired closely following deposition, when the bedding of these rocks was horizontal. To test this hypothesis one can rotate the magnetization directions to paleohorizontal, or “unfold” the rocks. The expectation if the magnetization predates tilting of the bedding is that directions will be least scattered upon correction to paleohorizontal. Both the Tauxe and Watson (1994) and the McElhinny (1964) fold tests were used to help constrain the age of magnetization in this way. The fold tests performed on second-component directions of the Sentinel Island Formation show significant results (Fig. 20) indicating maximum clustering of the directions between 30 and 80% unfolding. Fold tests performed on the ChRM60 components showed unimodal results and were best clustered at 40% and 50% unfolding (Table 5). Strong clustering of directions at less than 100% unfolding indicates that the Sentinel Island Formation may not retain magnetization acquired closely following deposition. However, inclinations are best grouped after tilt-correction coordinates using inclination-only methods (McFadden and Reid, 1982) (Table 4). The difference between the tilt-corrected coordinate system in which the directions are best



clustered for the directional fold tests and the inclination-only fold tests could be due to the effect of slump or fault block rotations. Such rotations would contribute to scattering of directions from the Sentinel Island Formation, and account for its apparent syn-folding magnetization. The mean inclination of  $82^\circ$  from the tilt-corrected second-removed components (Table 3) is steeper than the mean inclination of  $60\text{-}66^\circ$  (Table 4) from the inclination-only method and is consistent with the syn-folding results caused by apparent differential block rotation. If so, the inclination-only test is a better indicator of when, relative to folding, the Sentinel Island Formation was magnetized. The maximum clustering of the inclination-only test then indicates that these rocks still carry their original magnetization.

Fold tests for the Spieden Bluff Formation using all site means of the third-component directions did not show significant results for unfolding (Fig. 21). However, tilt corrected directions clustered better within sites 3 and 4 and significantly better within site 6. This increase in clustering suggests that magnetization was likely acquired prior to folding in the Spieden Bluff Formation (Fig. 22). The indeterminate fold test using site means could be the result of scatter produced by rotation of either slump or fault blocks. The ChRM70 and ChRM80 components cluster best at 100% unfolding (Table 9).

## 7.2 Inclination Error

Dickinson and Butler (1998) suggested that turbidites and other clastic marine sediments may have as much as  $25^\circ\text{-}30^\circ$  of inclination error. Inclination shallowing error in sediments is due to a mechanical process involving either alignment produced during deposition or alignment produced by compaction (see review by Tauxe, 1993). Each of these processes will result in a measurable mineral fabric with greater alignment

correlated with more intense fabric. To test for the possibility of inclination-shallowing in these sediments, the AMS results ( $1/P$ , or  $K_{\min}/K_{\max}$ ) were compared to the tangent of the inclination of individual specimens (Fig. 23). This approach is applicable to AMS data for samples with predominantly PSD and MD magnetite (Hodych et al., 1999). If there is a significant inclination error, it should be correlated with fabric intensity (Hodych et al., 1999). A plot of  $1/P$  verses inclination does not support such a correlation (Fig. 23), indicating that significant inclination-shallowing is unlikely.

## 8. DISCUSSION – TECTONIC IMPLICATIONS

The present location of the Spieden Group is at  $48.6^{\circ}$  N latitude and  $237^{\circ}$  E longitude (Fig. 24a). The directions expected for the Spieden Group at the time it formed if it had formed at its present location relative to the North American continent were calculated. Reference poles for North America were chosen that correspond as closely as possible in age to the formations of the Spieden Group, and that come from cratonal rocks. The Cretaceous still-stand pole ( $71.4^{\circ}$  N latitude,  $194.9^{\circ}$  E longitude), spanning 125-85 Ma, is the best current reference pole for the early Cretaceous Sentinel Island Formation (McEnroe, 1996, Van Fossen and Kent, 1992). The pole from the Brushy Basin Member of the Morrison Formation ( $68.3^{\circ}$  N latitude,  $156.2^{\circ}$  E longitude; Bazard and Butler, 1994), located on the Colorado Plateau, was used as a reference for the Jurassic Spieden Bluff Formation. The expected paleomagnetic direction calculated for the Cretaceous Sentinel Island Formation is  $D = 334.6^{\circ}$ ,  $I = 74^{\circ}$  (corresponding to an expected latitude of  $60^{\circ}$  N). The expected direction for the Jurassic Spieden Bluff Formation is  $D = 327.4^{\circ}$ ,  $I = 65.3^{\circ}$  (corresponding to an expected latitude of  $47^{\circ}$  N) (Fig. 24a and b).

The estimate of the original latitude for the Sentinel Island Formation is  $45.7^\circ$  N obtained using the mean inclination of  $64^\circ$  from the tilt-corrected inclination-only analysis of the paleomagnetic data (Table 4). This latitude does not match the expected latitude of  $60^\circ$  N and indicates these rocks may have been ca. 1500 km south of their present location with respect to North America during Early Cretaceous time. Upper and lower bounds of error using the  $\alpha_{95}$  of  $7.8^\circ$  ( $I = 56.2^\circ$  and  $71.9^\circ$ ) correspond to latitudes of  $36.8$  to  $56.8^\circ$  N (Fig. 24b). Although the Sentinel Island Formation rocks lack a meaningful correlation between magnetic fabrics and inclination, 10 degrees of compaction-flattening would eliminate the anomaly between the observed and expected paleolatitudes. Compaction flattening of inclination is more common in siltstones and shales with high clay-mineral content (Kodama and Sun, 1990). Given this tendency, compaction-flattening should be more pronounced in the finer-grained and more clay-rich Spieden Bluff Formation than in the coarser, more sand-rich Sentinel Island Formation. Considering both the sand-rich lithology and the lack of indication of compaction fabrics in the Sentinel Island Formation, the inclination determined from these rocks very likely is an accurate record of the latitude at which these rocks were deposited.

The mean inclination of  $65^\circ$  from tilt-corrected characteristic directions for the Jurassic Spieden Bluff Formation indicates that it originated at the latitude of  $47.0^\circ$  N. This latitude is in perfect agreement with the expected North American latitude of  $47^\circ$  N. Upper and lower bounds of error ( $I = 54.6^\circ$  and  $75.5^\circ$ ) correspond to latitudes of  $35.1^\circ$  N to  $62.7^\circ$  N (Fig. 24c).



The high paleolatitude of the Spieden Group is in marked disagreement with the only other paleomagnetic study of the San Juan Islands that has reported a primary remanence from a pre late-Cretaceous unit. Bogue et al. (1989) reported a primary remanence in the upper Jurassic James Island Formation, based on a complex three-stage tilt correction. The tilt-corrected remanence in those rocks has a shallow inclination, leading Bogue et al. (1989) to conclude that the clastic marine sediments of the James Island Formation were deposited at equatorial latitudes during late Jurassic time. If the paleolatitudes determined by both this study and that of Bogue et al. (1989) are reliable, then these two units have had very different displacement histories.

The remaining question regarding these rocks is where they were relative to the North American margin. Here are two likely scenarios. The first scenario is that the clastic sediments are a North American overlap sequence (Brandon et al., 1988; McClelland et al., 1992). If so, the concordant paleolatitude of the Upper Jurassic Spieden Bluff Formation would be consistent with accretion of the Haro Terrane to North America close to its present-day latitude. The Spieden Group would have then been translated 1500 km south along the coast by Valanginian time. A test for this would be to determine if the sediments that form the Spieden Group have a unique indicator of North American provenance, ideally one that may record a change in sediment source consistent with late Jurassic-early Cretaceous sinistral displacement. McClelland et al. (1992) summarizes several lines of evidence that suggest accretion of the Alexander-Wrangellia-Peninsular amalgamated terranes to the North American margin during the mid-Jurassic (prior to deposition of the Spieden Group). In their model, the Spieden Group is placed at the southern end of the arc complex on the Alexander-Wrangellia-

Peninsular terrane, with the Gambier arc being the most likely candidate for the source of the arc-derived clasts within the Spieden Group.

The second scenario assumes that these units were not yet accreted to North America and were moving in the Pacific Basin (Moores, 1998). A test for this would be to determine the provenance of the Spieden Group to be either an island arc or another continent, possibly Eurasia.

The position of the Spieden Group during the Early Cretaceous would constrain the timing of the early Cretaceous sinistral translation of the Insular Superterrane (Monger et al., 1994) if these rocks are correlative to similar sediments on Vancouver Island (Kyuquot Group) (Johnson, 1981). If this correlation is accurate, relatively southward displacement must have occurred prior to deposition of the oldest rocks in the Sentinel Island Formation, or Valanginian time. Placing the Haro Terrane 1500 km to the south prior to the Hauterivian is also in agreement with geological evidence for northward translation of other San Juan-North Cascades units (Decatur terrane and Shuksan Suite) during Hauterivian to Aptian time (Garver, 1988; Brown and Blake, 1987).

## **9. CONCLUSION**

Paleomagnetism was used to measure magnetic directions in the Spieden Group. Three directions of magnetization are present in most of the Spieden Bluff Formation specimens and two directions are present in most of the specimens from the Sentinel Island Formation. Fold tests performed on the Sentinel Island second-removed components have a maximum clustering of directions at less than 100% unfolding, indicating magnetization may have been acquired during folding. Fold tests performed on

the inclination-only directions showed best grouping at 100% unfolding. The difference in the results between the fold tests suggests the scattering of directions at less than 100% unfolding may be due to block fault movement or rotations. Rocks of the upper Jurassic Spieden Bluff Formations have more complex magnetizations. Based upon improved clustering of directions from several individual sites after structural correction, the magnetization recorded by the rocks is also most likely primary (Late Jurassic in age).

A latitude of 60° N was calculated from the expected paleomagnetic directions that the Sentinel Island Formation should have had if it had been at its current location with respect to North America during the Early Cretaceous. The calculated latitude of origin from paleomagnetic directions for the Cretaceous Sentinel Island Formation is 45.7° N (obtained using inclination-only data with a mean inclination of 64°) indicating the rocks were 1500 km to the south of their current location with respect to North America during early Cretaceous time. The latitude of 47° N was calculated from the expected paleomagnetic directions that the Spieden Bluff Formation should have had if it had been at its current location with respect to North America in the Late Jurassic. The calculated latitude of origin from the Jurassic Spieden Bluff Formation paleomagnetic directions is 47° N indicating that it either has remained in its present location since its deposition, or has been translated and returned to its original latitude. Combined, the directions obtained from both formations indicate the Haro Terrane was translated south 1500 km between Late Jurassic and Early Cretaceous time. These results agree well with prior structural and tectonic models that have suggested sinistral motion of terranes off shore of the North American margin for this time period.



## 10. REFERENCES CITED

- Bazard, D. R. and R. F. Butler, Paleomagnetism of the Brushy Basin Member of the Morrison Formation: Implications for Jurassic apparent polar wander, *J. Geophys. Res.*, 99, 6695-6710, 1994.
- Beck, M. E., Discordant paleomagnetic poles positions as evidence of regional shear in the western Cordillera of North America, *Am. J. Sci.*, 276, 694-712, 1976.
- Beck, M. E., Paleomagnetism of continental North America; Implications for displacement of crustal blocks within the Western Cordillera, Baja California to British Columbia, *Geol. Soc. Am. Bull.*, 172, 471-492, 1989.
- Bogue, S. W., D. S. Cowan and J. I. Garver, Paleomagnetic evidence for poleward transport of Upper Jurassic rocks in the Decatur Terrane, San Juan Islands, Washington, *J. Geophys. Res.*, 94, 10415- 10427, 1989.
- Briden, J.C., and Ward, M.A., Analysis of magnetic inclination in borecores, *Pure and App. Geophys.*, v. 63, p. 133-152, 1962.
- Brandon, M. T., D. S. Cowan and J. A. Vance, The Late Cretaceous San Juan thrust System, San Jan Islands, Washington, *Spec. Pap. Geol. Soc. Am.*, 221, 82 pp., 1988.
- Brown, E. H., M. C. Blake, Correlation of Early Cretaceous Blueschists in Washington, Oregon, and Northern California, *Tectonics*, 6, 795-806, 1987.
- Burmester, R. F., M. C. Blake Jr. and D. C. Engebretson, Remagnetization during the Cretaceous Normal Superchron in Eastern San Juan Islands, WA: implications for tectonic history, *Tectonophysics*, 326, 73-92, 2000.
- Channell, J. E. T. and C. McCabe, Comparison of magnetic hysteresis parameters of unremagnetized and remagnetized limestones, *J. Geophys. Res.*, 99, 4613-4623, 1994.
- Day, R., M. Fuller and V. A. Schmidt, Hysteresis properties of titanomagnetites: grain-size and compositional dependence, *Phys. Earth Planet. Int.*, 13, 260-267, 1977.
- Dickinson, W. R. and R. E. Butler, Coastal and Baja California paleomagnetism reconsidered, *Geol. Soc. Am. Bull.*, 110, 1268-1280, 1998.
- Dunlop, D. and O. Ozdemir, *Rock Magnetism: Fundamentals and Frontiers*, Cambridge University Press, 1997, 573 pp.

- Engebretson, D. C., A. Cox, and R. G. Gordon, Relative motions between oceanic and continental plates in the Pacific basin, *Spec. Pap. Geol. Soc. Am.*, 206, 1985.
- England, T.D.J. and T.J. Calon, The Cowichan fold and thrust system, Vancouver Island, southwestern British Columbia, *Geol. Soc. Am. Bull.*, 103, 336-362, 1991.
- Enkin, R. J., J. Baker and P. S. Mustard, Paleomagnetism of the Upper Cretaceous Nanaimo Group, Southwestern Canadian Cordillera, *Can. J. Earth Sci.*, 38, 1387-1401, 2001.
- Fisher, R. A., Dispersion on a sphere, *Proc. R. Soc. London, Ser. A*, 217, 295-305, 1953.
- Garver, J. I., Fragment of the Coast Range Ophiolite and the Great Valley Sequence in the San Juan Islands, Washington, *Geology*, 16, 948-951, 1988.
- Haggart, J. W., Paleontological Report, *Geol. Survey of Can.*, JWH-2000-05, 1-3, 2000.
- Hodych, J. P., S. Bijaksana and R. Patzold, Using magnetic anisotropy to correct for paleomagnetic inclination shallowing in some magnetite-bearing deep-sea turbidites and limestones, *Tectonophysics*, 307, 191-205, 1999.
- Housen, B, Shriver, T., Knowles, A., Burgess, M., Chase, M., Fawcett, T., Hults, C., Kenshalo, S., Transport magnetostratigraphy: Preliminary results from the Cretaceous Nanaimo Group; *Eos, Transactions, Am. Geophys. Union*, 79, Suppl., 73, 1998.
- Hults, C. K. and B. A. Housen, Low temperature chemical remagnetization of the Haro Formation, San Juan Islands, Washington, *Geol. Soc. Am. Abstr. Programs*, 36, no. 6, A-20, 2000.
- Irving, E., Paleopoles and paleolatitudes of North America and speculations about displaced terrains, *Can. J. Earth Sci.*, 16, 669-694, 1979.
- Johnson, S. Y., The Spieden Group: an anomalous piece of the Cordilleran paleogeographic puzzle, *Can. J. Earth Sci.*, 18, 1694-1707, 1981.
- Kirschvink, J. L., The least squares line and plane and the analysis of paleomagnetic data, *Geophys. J. R. Astron. Soc.*, 62, 699-718, 1980.
- Kodama, K.P. and W.W. Sun, SEM and magnetic fabric study of a compacting sediment, *Geophys. Res. Lett.*, 17, 795-798, 1990.
- May, S. R., and R. F. Butler, North American Jurassic apparent polar wander: implications for plate motion, paleogeography, and Cordilleran tectonics: *J. Geophys. Res.*, 91, 11519-11544, 1989.



- McClellan, R.D., The geology of the San Juan Islands, University of Washington, *Publications in Geology*, 2, 185 p. 1927.
- McClelland, W. C., G. E. Gehrels and J. B. Saleeby, Upper Jurassic-Lower Cretaceous Basin Strata along the Cordilleran Margin: implications for Accretionary History of the Alexander-Wrangellia-Peninsular Terrane, *Tectonics*, 11, 823-835, 1992.
- McFadden, P.L., and A.B. Reid, Analysis of paleomagnetic inclination data, *Geophys. J. R. Aston. Soc.*, 69, 307-319, 1982.
- McElhinney, M. W., Statistical significance of the fold test in paleomagnetism, *Geophys. J. R. Aston. Soc.*, 8, 338-340, 1964.
- McEnroe, S. A. A Barremian-Aptian (Early Cretaceous) North American paleomagnetic reference pole, *J. Geophys. Res.*, 101, 15,819-15,836, 1996.
- Misch, P., Tectonic evolution of the North Cascades of Washington state: A west-Cordilleran case history, *Spec. Vol. 8*, pp. 101-148, Can. Inst. Min. Metall., Montreal, 1966.
- Monger, J. W. H., P. van der Heyden, J. M. Journeay, C. A. Evenchick and J. B. Mahoney, Jurassic-Cretaceous basins along the Canadian Coast Belt: Their bearing on pre-mid-Cretaceous sinistral displacements, *Geology*, 22, 175-178, 1994.
- Moore, E.M., Ophiolites, the Sierra Nevada, "Cordillera," and orogeny along the Pacific and Caribbean margins of North and South America, *International Geology Rev.*, 40, 40-54, 1998
- Tauxe, L., *Paleomagnetic Principles and Practice*, Kluwer Academic Publications, 1998, 299pp.
- Tauxe, L., Sedimentary records of relative paleointensity of the geomagnetic field: theory and practice, *Rev. Geophys.* 31, 319-354, 1993.
- Tauxe, L. and G. Watson, The fold test: an eigen analysis approach, *Earth Planet. Sci. Lett.*, 122, 331-341, 1994.
- van Damme, D., A new method to determine paleosecular variation, *Phys. Earth Plan. Int.*, 85, 131-142, 1994.
- Van Fossen, M. C., and D. V. Kent, Paleomagnetism of 122 Ma plutons in New England and mid-Cretaceous paleomagnetic field in North America: true polar wander or large-scale differential mantle motion? *J. Geophys. Res.*, 97, 19,651-19,661, 1992.

- Ward, P. D., J. M. Hurtado, J. L. Kirschvink, and K. L. Verosub, Measurements of the Cretaceous Paleolatitude of Vancouver Island: Consistent with the Baja-British Columbia Hypothesis, *Science*, 277, 1642-1645, 1997.
- Whetten, J. T., D. L. Jones, D. S. Cowen, and R. E. Zartman, Ages of Mesozoic terranes in the San Juan Islands, Washington, in Mesozoic paleogeography of the western United States, edited by D. G. Howell and K. McDougall, *Soc. Econ. Paleontol. Mineral., Spec. Publ. 2*, 117-128, 1978.
- Whetten, J. T., R. E. Zartman, R. J. Blakely, and D. L. Jones, Allochthonous Jurassic ophiolite in northwest Washington, *Geol. Soc. Am. Bull.*, 91, 359-368, 1980.
- Zijderveld, J. D. A., A. C. Demagnetization of rocks: Analysis of results, in *Methods in Paleomagnetism*, edited by D. W. Collinson, K. M. Creer, and S. K. Runcorn, pp. 254-286, Elsevier, New York, 1967.

Table 1. Fossil and fossil assemblages of the Lower Cretaceous Sentinel Island Formation lower member

Identification by Jim Haggart of the Geological Society of Canada, 2000.

Fossils submitted:	Age	Paleogeographic constraint
Inoceramus cf. paraketzovi –	Valanginian to Hauterivian	western Canadian Cordillera, western British Columbia, Alaska, northeast Russia,
Homolomites stantoni –	middle to early Hauterivian	boreal/North temperate, west coast of North America (northern California to the Canadian Arctic), Greenland
Lytoceratid ammonite - indeterminate	-----	
Bivalves - probably related to Buchia crassicollis	uppermost Valanginian	
Bivalves - indeterminate	-----	
Inoceramid bivalve shell prisms	-----	

Table 2. Site-averaged paleomagnetic data of the first-removed component for the Sentinel Island Formation  
(MAD <20)

Site	N/N <sub>0</sub>	In-situ				Tilt-corrected			
		D (deg)	I (deg)	k	α95 (deg)	D (deg)	I (deg)	k	α95 (deg)
98Ksi14	5/7	31.2	65.3	3	59.6	216.2	60.2	7	32.3
00Ksi15	5/5	346.4	84.7	37	12.8	210.1	49.0	37	12.8
00Ksi16	3/5	55.9	69.6	159	9.8	200.8	43.3	159	9.8
00Ksi19	4/10	5.4	58.7	4	53.8	198.3	57.4	4	51.9
00Ksi20	8/14	137.0	48.8	6	25.5	190.8	50.8	6	25.8
Mean:		55.4	75.0	10	25.2	202.8	52.5	82	8.5

Table 3. Site-averaged paleomagnetic data of the second-removed component for the Sentinel Island Formation  
(MAD <20)

Site	N/N <sub>0</sub>	In-situ				Tilt-corrected			
		D (deg)	I (deg)	k	α95 (deg)	D (deg)	I (deg)	k	α95 (deg)
98Ksi13	8/8	28.2	47.3	165.1	4.3	201.4	52.7	166.4	4.3
98Ksi14	7/7	32.9	22.2	32.6	10.7	187.6	77.0	32.6	10.7
00Ksi15	5/5	29.1	38.7	35.0	13.1	47.9	82.7	38.9	12.4
00Ksi16	4/5	14.6	50.7	5.7	42.1	235.0	61.0	5.7	42.1
00Ksi17	5/5	47.5	52.4	36.5	12.8	102.9	78.9	36.6	12.8
00Ksi18	4/4	28.9	68.0	22.7	19.7	212.1	79.0	22.8	19.7
00Ksi19	9/10	39.4	22.6	153.1	4.2	98.3	64.7	147.0	4.3
00Ksi20	14/14	49.4	47.7	9.6	13.6	358.8	80.6	8.1	14.9
Mean:		34.1	44.2	22.1	12.0	182.5	81.8	16.2	14.2

Notes: N<sub>0</sub> is the number of specimens measured, N is the number of specimens used in the averages calculated. The mean direction is given by its declination (D), inclination (I), radius of 95% cone of confidence (α95), and precision parameter (k) [Fisher, 1953].

Table 4. Inclination-only data - Incremental unfolding of paleomagnetic data using intensity-selected characteristic components for the Sentinel Island Formation

In-situ						
intensity component	I (deg)	bounds		N	k	$\alpha_{95}$ (deg)
		upper (deg)	lower (deg)			
ChRM50	35.6	51.9	19.3	4	54	16.3
ChRM60	45.6	56.7	34.5	10	20	11.1
ChRM70	38.1	55.3	21.0	9	10	17.1
ChRM80	40.1	49.8	30.3	18	13	9.8
ChRM90	27.6	57.1	-2.0	3	50	29.5

Tilt-corrected						
intensity component	I (deg)	bounds		N	k	$\alpha_{95}$ (deg)
		upper (deg)	lower (deg)			
ChRM50	59.2	106.9	11.5	4	7	47.7
ChRM60	result no good					
ChRM70	64.0	71.9	56.2	9	46	7.9
ChRM80	result no good					
ChRM90	65.9	88.8	43.0	3	82	22.9

Notes: N is the number of specimens used in the averages calculated. The mean direction is given by its declination (D), inclination (I), radius of 95% cone of confidence ( $\alpha_{95}$ ), and precision parameter (k) [Fisher, 1953].



Table 5. Incremental unfolding of paleomagnetic data using intensity selected characteristic components for the Sentinel Island Formation

% unfolding	ChRM60					ChRM70				
	D (deg)	I (deg)	$\alpha_{95}$ (deg)	N	k	D (deg)	I (deg)	$\alpha_{95}$ (deg)	N	k
-40	43.6	30.8	18.7	20	4	36.8	33.6	48.6	9	2
-30	44.1	36.7	18.5	20	4	33.8	30.2	30.4	9	4
-20	39.7	35.3	9.1	20	14	34.3	36.2	30.2	9	4
-10	40.2	41.6	8.6	20	15	35.0	42.1	30.0	9	4
0	40.8	47.7	8.1	20	17	41.2	38.9	13.8	9	15
10	41.8	53.8	7.7	20	19	42.8	45.0	13.2	9	16
20	43.3	59.8	7.3	20	21	45.0	51.1	12.8	9	17
30	45.5	65.7	7.0	20	22	48.2	57.0	12.4	9	18
40	49.3	71.5	6.9	20	23	53.0	62.7	12.2	9	19
50	56.4	77.1	6.9	20	24	60.3	68.1	12.1	9	19
60	73.5	82.2	7.0	20	23	72.2	72.9	12.2	9	19
70	302.4	85.0	7.3	20	21	271.8	76.4	12.4	9	18
80	352.4	82.3	7.7	20	19	299.0	77.4	12.8	9	17
90	10.0	77.3	8.3	20	17	324.2	75.4	13.3	9	16
100	17.3	71.7	8.9	20	14	341.0	71.4	13.9	9	15
110	21.3	66.0	9.7	20	12	351.0	66.3	14.5	9	14
120	23.7	60.2	10.5	20	11	357.3	60.7	15.3	9	12
130	25.4	54.3	11.4	20	9	1.4	54.9	16.2	9	11
140	26.7	48.3	12.3	20	8	4.2	48.8	17.1	9	10

% unfolding	ChRM80				
	D (deg)	I (deg)	$\alpha_{95}$ (deg)	N	k
-40	36.9	32.7	24.9	18	3
-30	37.3	32.9	19.3	18	4
-20	34.6	33.9	13.7	18	7
-10	34.2	39.2	13.2	18	8
0	33.9	44.4	12.8	18	8
10	33.5	49.6	12.4	18	9
20	33.2	54.7	12.2	18	9
30	32.8	59.7	12.1	18	9
40	32.3	64.8	12.1	18	9
50	31.6	69.8	12.2	18	9
60	30.6	74.7	12.5	18	9
70	28.5	79.7	12.9	18	8
80	22.3	84.7	13.5	18	8
90	313.6	83.9	13.6	18	7
100	349.4	81.5	14.1	18	7
110	6.1	77.4	14.7	18	7
120	14.3	72.8	15.4	18	6
130	19.1	67.9	16.2	18	6
140	22.3	62.9	17.1	18	5

Notes: N is the number of specimens used in the averages calculated. The mean direction is given by its declination (D), inclination (I), radius of 95% cone of confidence ( $\alpha_{95}$ ), and precision parameter (k) [Fisher, 1953].

Table 6. Site-averaged paleomagnetic data of the first-removed component for the Spieden Bluff Formation  
(MAD <20)

Site	N/N <sub>o</sub>	In-situ				Tilt-corrected			
		D (deg)	I (deg)	k	α95 (deg)	D (deg)	I (deg)	k	α95 (deg)
98Jsb01	9/9	34.7	72.3	4	30.4	43.2	67.7	6	3.1
99Jsb04	9/11	30.8	87.3	18	12.5	299.1	78.7	8	7.7
99Jsb05	7/10	186.6	66.0	2	56.2	299.7	78.0	4	1.9
99Jsb06	6/10	329.9	77.4	4	37.6	322.2	85.1	4	3.0
99Jsb07	3/3	23.5	50.1	9	44.2	24.9	55.0	3	8.9
99Jsb08	24/26	52.6	71.9	10	10.0	48.4	60.0	20	5.2
99Jsb09	3/10	53.9	64.0	9	42.6	56.3	46.7	8	48.4
Mean		39.0	77.5	16	15.5	30.4	71.9	16	15.6

Table 7. Site-averaged paleomagnetic data of the second-removed component for the Spieden Bluff Formation  
(MAD <20)

Site	N/N <sub>o</sub>	In-situ				Tilt-corrected			
		D (deg)	I (deg)	k	α95 (deg)	D (deg)	I (deg)	k	α95 (deg)
99Jsb04	10/11	317.8	28.3	8	18.1	301.9	34.2	2	45.6
99Jsb05	9/10	48.8	72.7	2	46.5	139.3	82.5	2	48.5
99Jsb08	15/26	249.7	84.7	3	28.2	271.4	84.0	3	29.4
Mean		330.9	68.9	5	62.4	295.3	72.6	6	55.2

Notes: N<sub>o</sub> is the number of specimens measured, N is the number of specimens used in the averages calculated. The mean direction is given by its declination (D), inclination (I), radius of 95% cone of confidence (α95), and precision parameter (k) [Fisher, 1953].

Table 8. Site-averaged paleomagnetic data of the third-removed component for the Spieden Bluff Formation

(MAD <20)

Site	N/No	In-situ				Tilt-corrected			
		D (deg)	I (deg)	k	$\alpha_{95}$ (deg)	D (deg)	I (deg)	k	$\alpha_{95}$ (deg)
98Jsb01	7/9	147.0	44.6	14	17.0	124.0	53.3	10	19.6
98Jsb03	4/5	328.6	79.5	31	16.8	47.0	67.8	38	15.1
99Jsb04	4/11	121.7	42.7	6	40.3	121.7	50.0	8	34.6
99Jsb06	4/10	338.7	65.9	3	70.6	39.8	56.8	4	56.8
99Jsb07	3/3	355.4	71.4	52	17.4	343.8	75.8	62	15.7
99Jsb08	25/26	302.5	82.1	7	12.3	31.5	78.5	5	14.1
99Jsb09	9/9	54.1	73.2	5	24.6	87.3	68.9	4	30.7

Mean      82.5      82.0      8      23.0      78.3      71.3      14      16.9

Notes:  $N_0$  is the number of specimens measured, N is the number of specimens used in the averages calculated. The mean direction is given by its declination (D), inclination (I), radius of 95% cone of confidence ( $\alpha_{95}$ ), and precision parameter (k) [Fisher, 1953].



Table 9. Incremental unfolding of paleomagnetic data using intensity-selected characteristic components for the Spieden Bluff Formation

% unfolding	ChRM60					ChRM70				
	D (deg)	I (deg)	$\alpha_{95}$ (deg)	N	k	D (deg)	I (deg)	$\alpha_{95}$ (deg)	N	k
-40	36.1	70.1	22.1	9	6	71.9	86.2	23.2	10	5
-30	37.3	69.5	20.8	9	7	72.5	86.9	23.4	10	5
-20	38.5	68.8	19.7	9	8	74.6	87.7	23.8	10	5
-10	39.7	68.2	18.7	9	9	81.3	88.5	24.4	10	5
0	40.9	67.6	17.9	9	9	292.0	89.2	25.2	10	5
10	42.2	66.9	17.2	9	10	13.1	89.1	26.1	10	4
20	43.4	66.3	16.8	9	10	35.8	88.0	27.2	10	4
30	44.6	65.6	16.6	9	11	41.7	86.6	28.4	10	4
40	45.9	64.9	16.6	9	11	44.1	85.0	29.6	10	4
50	47.2	64.1	16.9	9	10	46.6	69.1	25.3	10	5
60	48.3	63.3	17.4	9	10	46.7	68.1	24.1	10	5
70	49.6	62.4	18.0	9	9	47.0	67.2	23.0	10	5
80	50.7	61.5	18.9	9	8	47.4	66.4	22.1	10	6
90	51.8	60.5	19.9	9	8	47.8	65.7	21.4	10	6
100	52.9	59.3	21.1	9	7	48.2	65.0	20.9	10	6
110	54.0	58.2	22.4	9	6	48.6	64.5	20.7	10	6
120	55.0	56.9	23.8	9	6	49.1	63.8	20.7	10	6
130	55.9	55.5	25.3	9	5	49.6	63.3	21.0	10	6
140	56.8	54.0	26.9	9	5	50.2	62.7	21.5	10	6

% unfolding	ChRM80				
	D (deg)	I (deg)	$\alpha_{95}$ (deg)	N	k
-40	359.4	79.1	24.2	8	6
-30	5.1	77.0	21.7	8	8
-20	9.2	75.0	19.3	8	9
-10	12.3	72.9	17.1	8	11
0	14.7	70.9	15.1	8	14
10	16.7	68.9	13.3	8	18
20	18.3	67.0	11.8	8	23
30	19.8	65.0	10.8	8	27
40	21.2	63.1	10.4	8	30
50	22.5	61.2	10.5	8	29
60	23.8	59.2	11.2	8	25
70	25.1	57.2	12.4	8	21
80	26.3	55.2	14.0	8	17
90	27.6	53.1	15.8	8	13
100	28.9	51.0	17.8	8	11
110	30.2	48.9	19.8	8	9
120	43.9	60.4	33.2	8	4
130	45.1	59.0	33.2	8	4
140	46.0	57.4	33.4	8	4

Notes: N is the number of specimens used in the averages calculated. The mean direction is given by its declination (D), inclination (I), radius of 95% cone of confidence ( $\alpha_{95}$ ), and precision parameter (k) [Fisher, 1953].

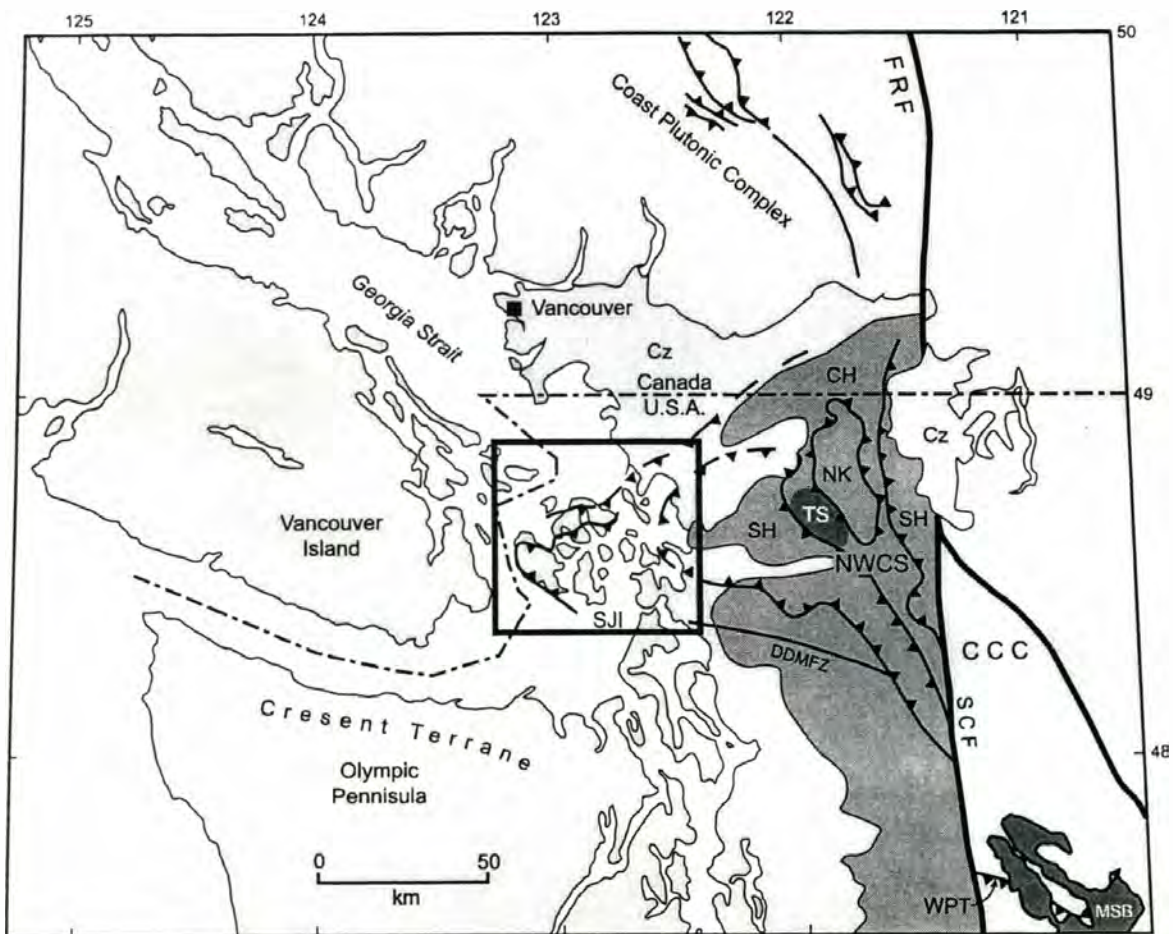


Figure 1. Location map of the San Juan Islands (SJI) relative to Vancouver Island, Coast Plutonic Complex, and the Northwest Cascades System (NWCS). From Burmester et al. (2000).

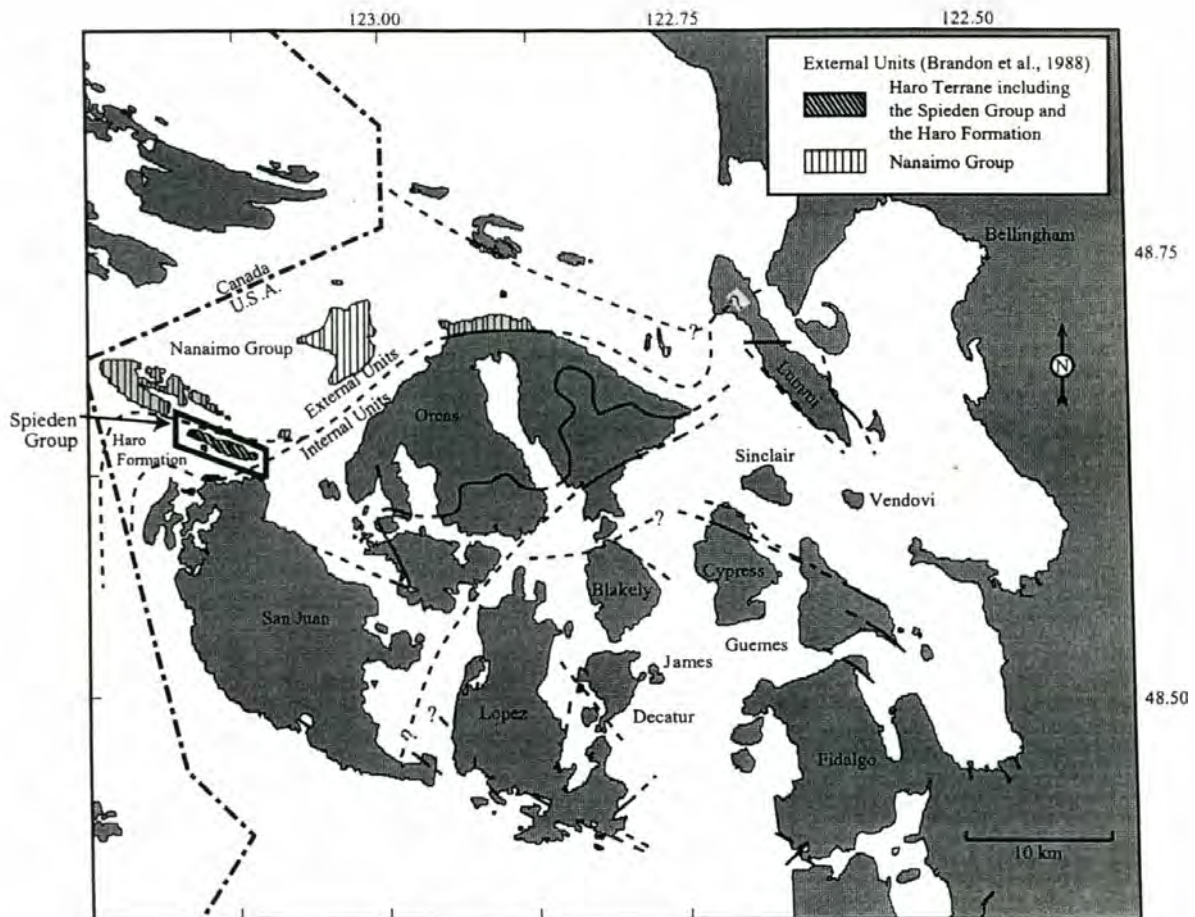


Figure 2. Location map for the faults and geographic names in the San Juan Islands. Modified after Burmester et al. (2000). Internal units include Orcas, San Juan and all other islands to the southeast. External units are to northwest. Dashed lines indicate faults and boundaries between terranes. Some fault traces taken from Brandon et al. (1988). Patterns in legend show the Haro Terrane and the Nanaimo Group.



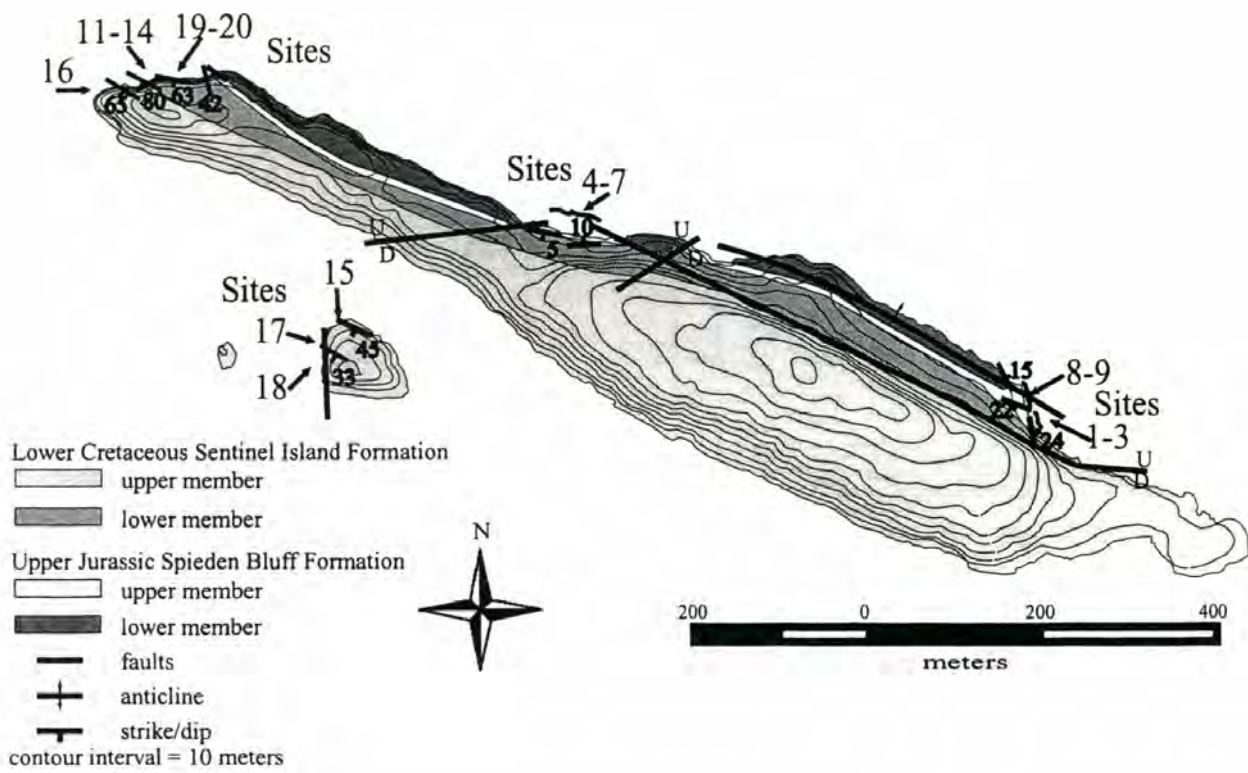


Figure 3. Location of paleomagnetic sites and geology of the Spieden Group. Modified after Johnson (1981).

AGE	GROUP	FORMATION	MEMBER	THICKNESS	LITHOLOGY	DESCRIPTION	
Early Cretaceous	Hauterivian	Spieden Group	Sentinel Island Formation	Upper member	600 m +	not exposed	Crudely stratified volcanic conglomerate and minor sandstone
Late Jurassic	Oxfordian or Kimmeridgian	Spieden Bluff Formation	Lower member	140 m		Unconformity Massive and thinly bedded fossiliferous sandstone and siltstone	
			Upper member	20 m		Unconformity Massive and thinly bedded fossiliferous sandstone and siltstone	
	Valanginian						
			Lower member	80 m	not exposed	Massive and crudely stratified volcanic breccia and conglomerate, minor sandstone, siltstone and tuff	

Figure 4. Stratigraphy of the Spieden Group. Modified after Johnson (1981).

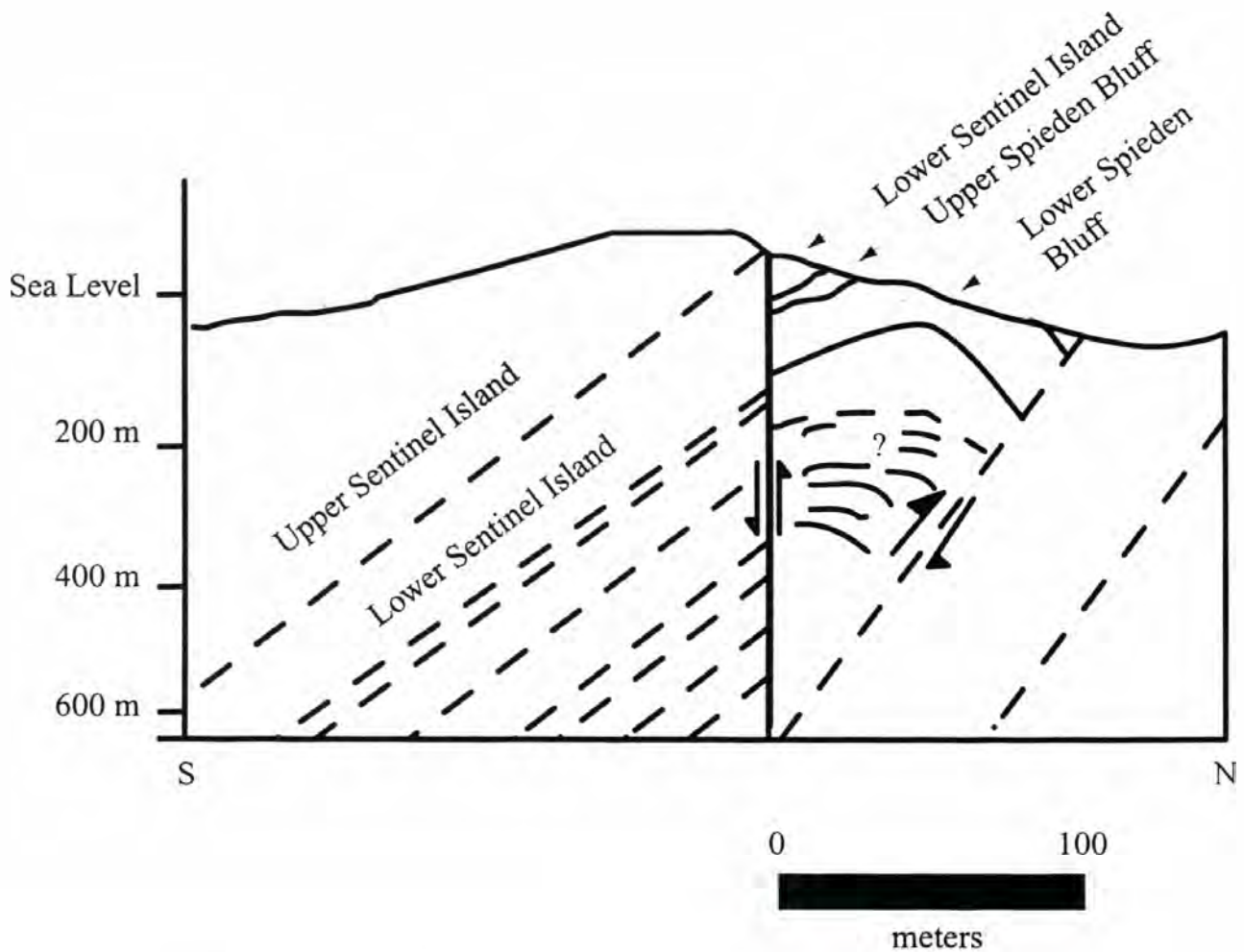


Figure 5. Cross-section showing general structures and inferred block movement within the Spieden Group. The Sentinel Island Formation has steeply tilted bedding. The Spieden Bluff Formation is gently folded. The Spieden Bluff Formation is inferred to be thrust up with respect to the Sentinel Island Formation. Modified after Johnson (1981).



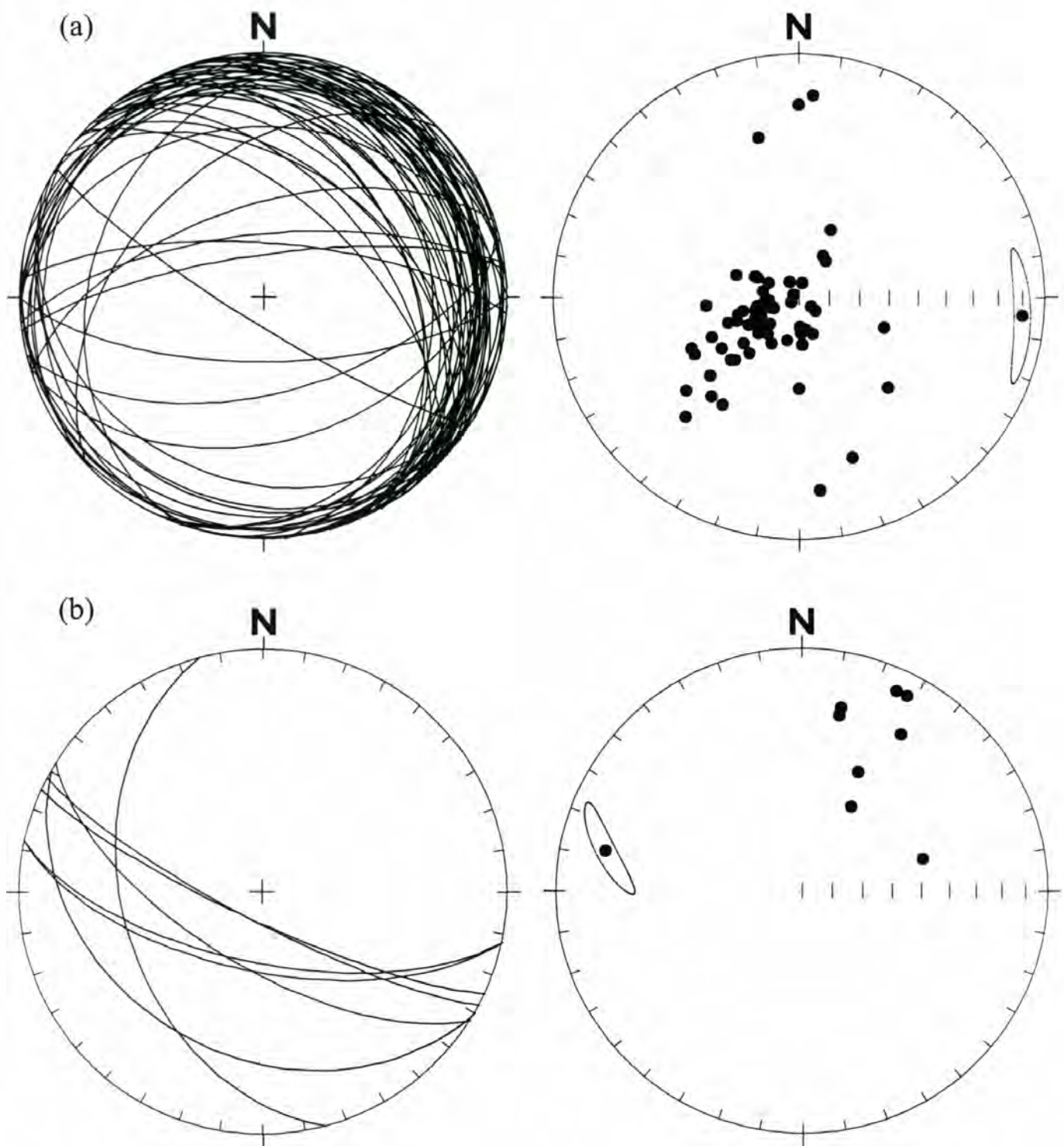


Figure 6. Equal area plots showing bedding planes represented by lines (left) and fold axes determined from the mean intersection of poles to bedding (right) for (a) Jurassic Spieden Bluff Formation and (b) Cretaceous Sentinel Island Formation.



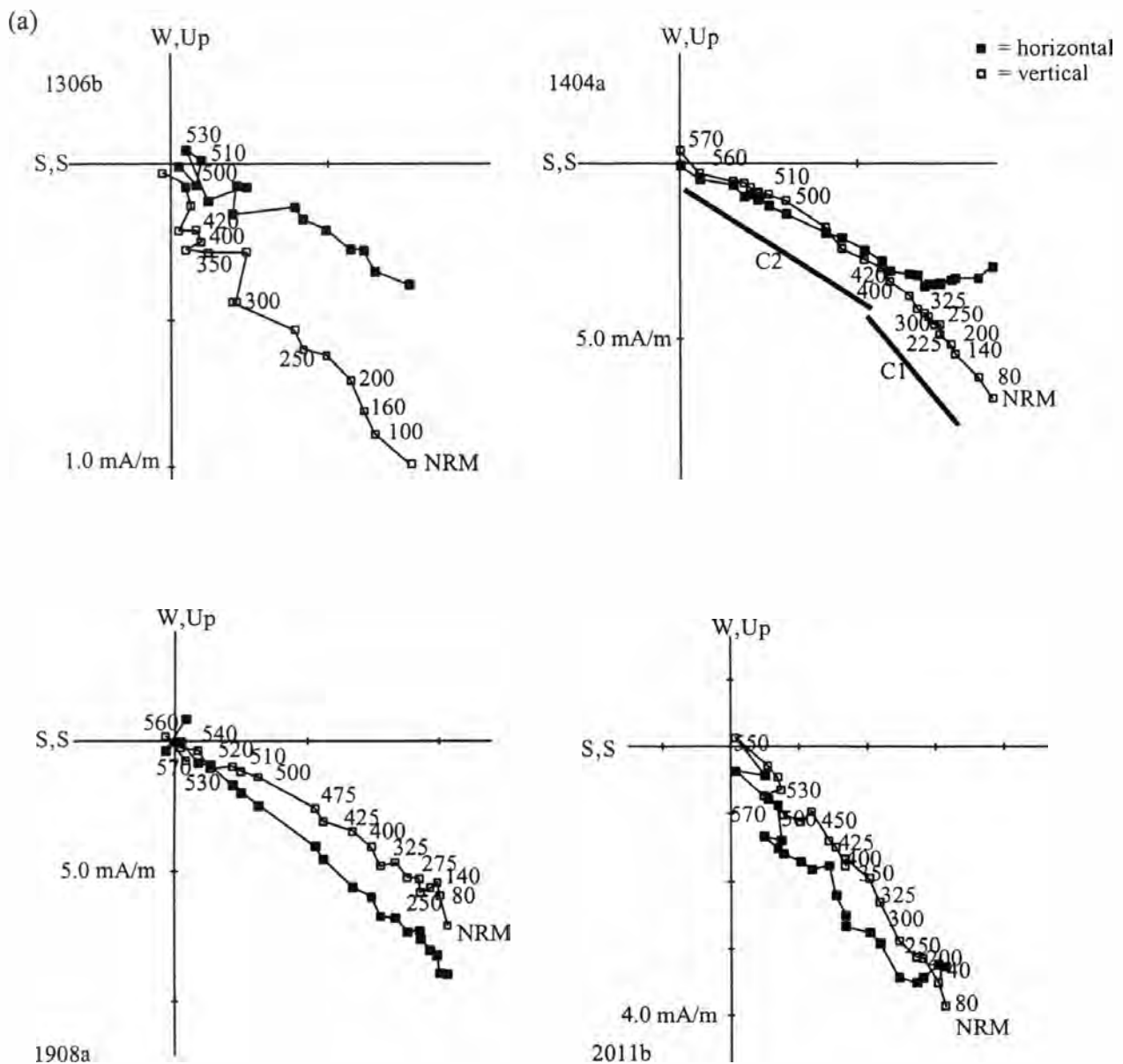


Figure 7. Representative demagnetization diagrams showing two components (C1 and C2) unblocking at  $\sim 300$  °C and  $\sim 500$  to  $580$  °C respectively for each site in the (a) lower and (b) upper Sentinel Island Formation.

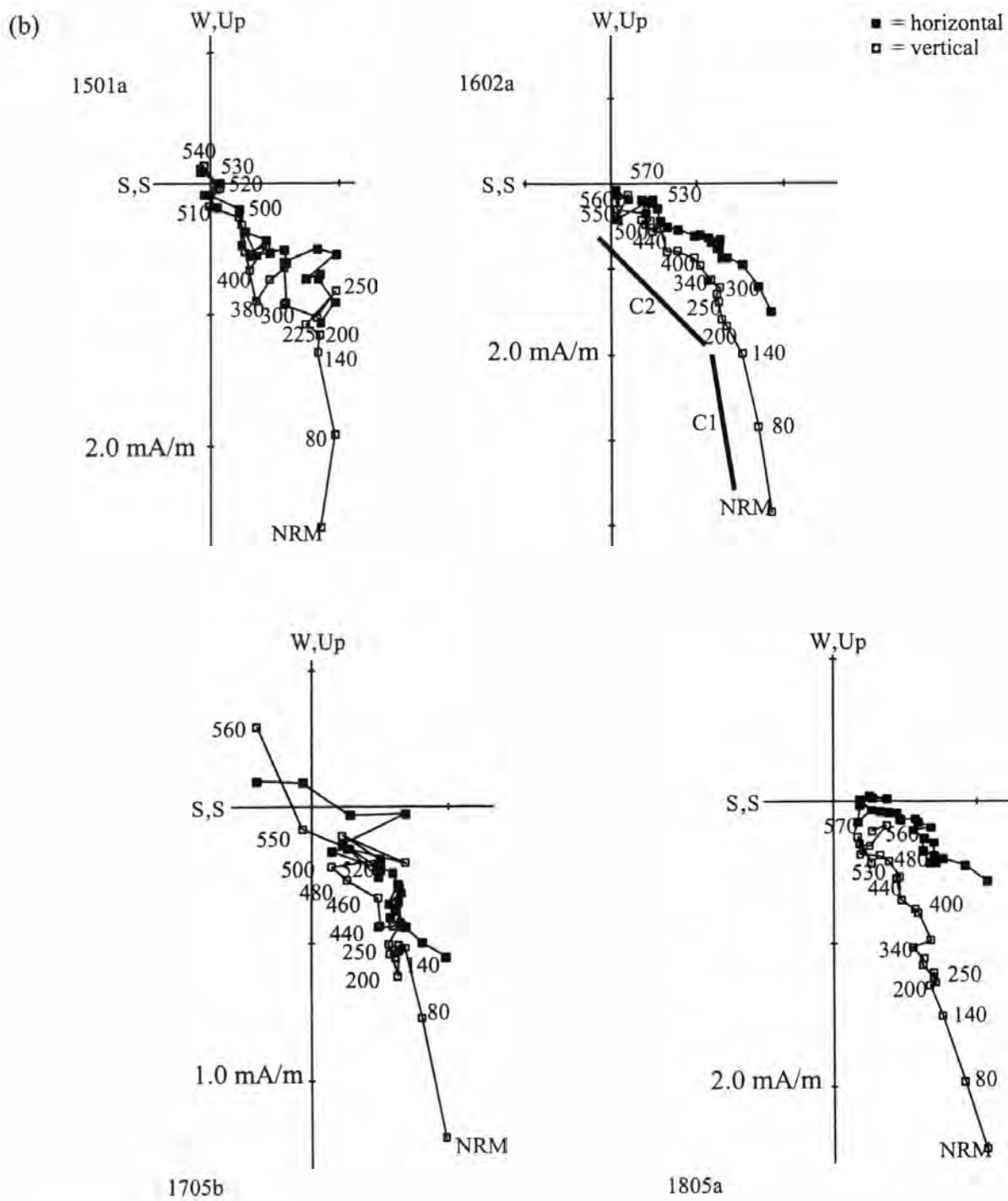


Figure 7. continued

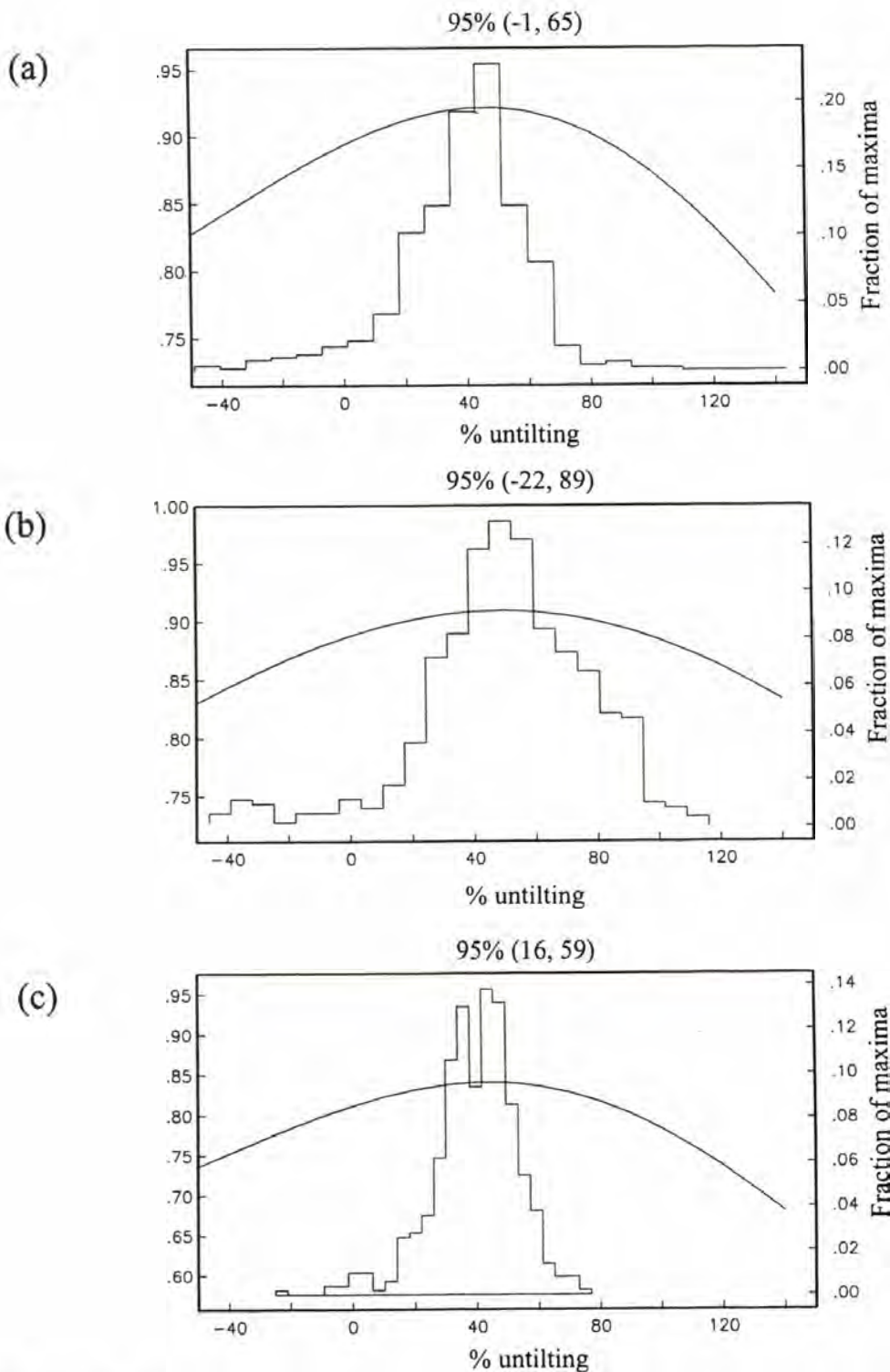


Figure 8. Incremental unfolding of the Cretaceous Sentinel Island Formation using characteristic components after 10% increments of intensity. This process was performed by grouping components by the ratio of intensity of the component removed to the total intensity. Constraints required for the 95% confidence interval are located above each plot. Components with line segments of (a) ChRM60 (60-70%), (b) ChRM70 (70-80%) and (c) ChRM80 (80-90%) of the total intensity. Bootstrap method of Tauxe and Watson (1994).

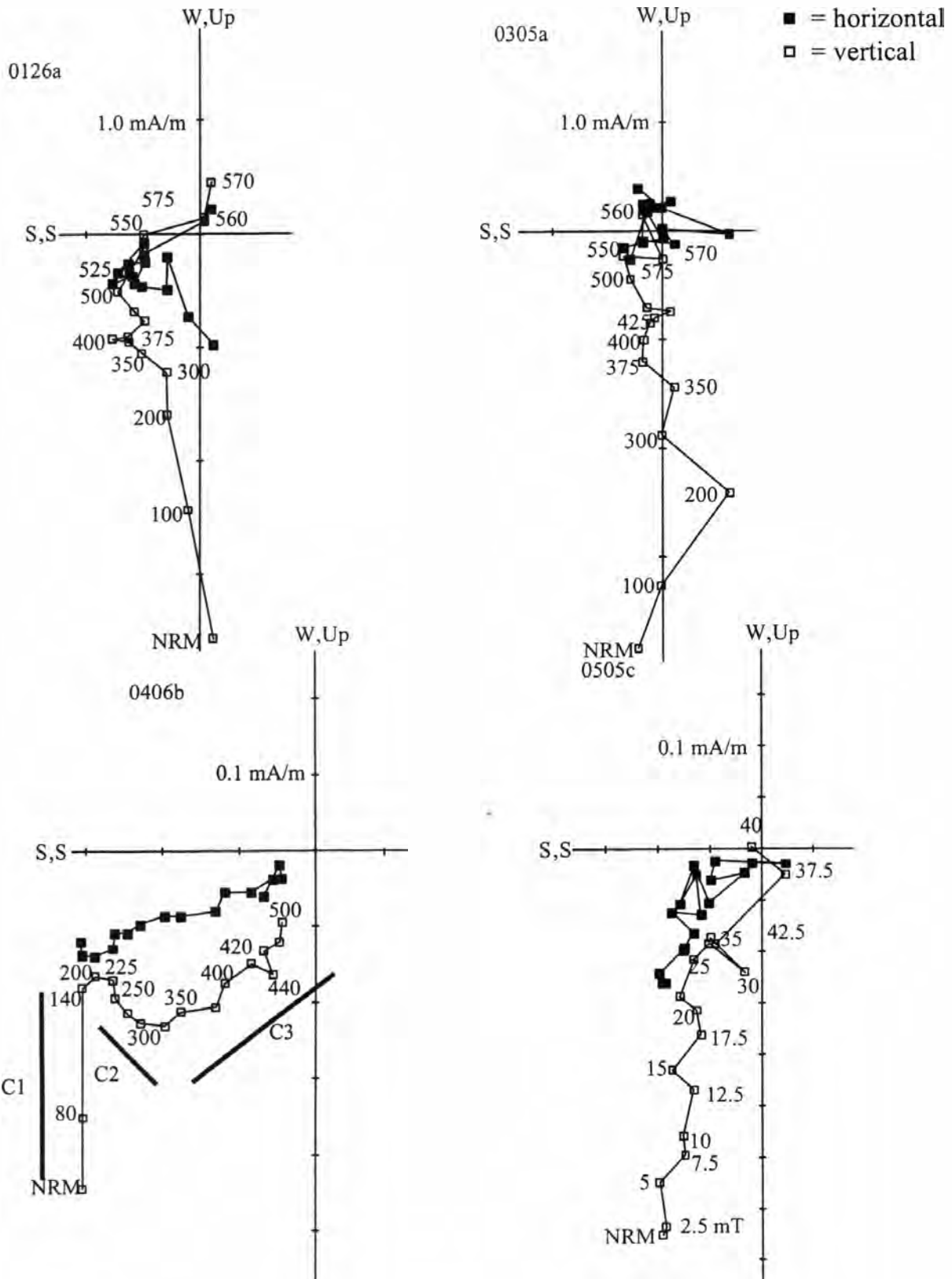


Figure 9. Representative demagnetization diagrams showing three components (C1, C2 and C3) unblocking at  $\sim 200$  °C,  $\sim 400$  °C and  $\sim 580$  °C for sites in the Spieden Bluff Formation.

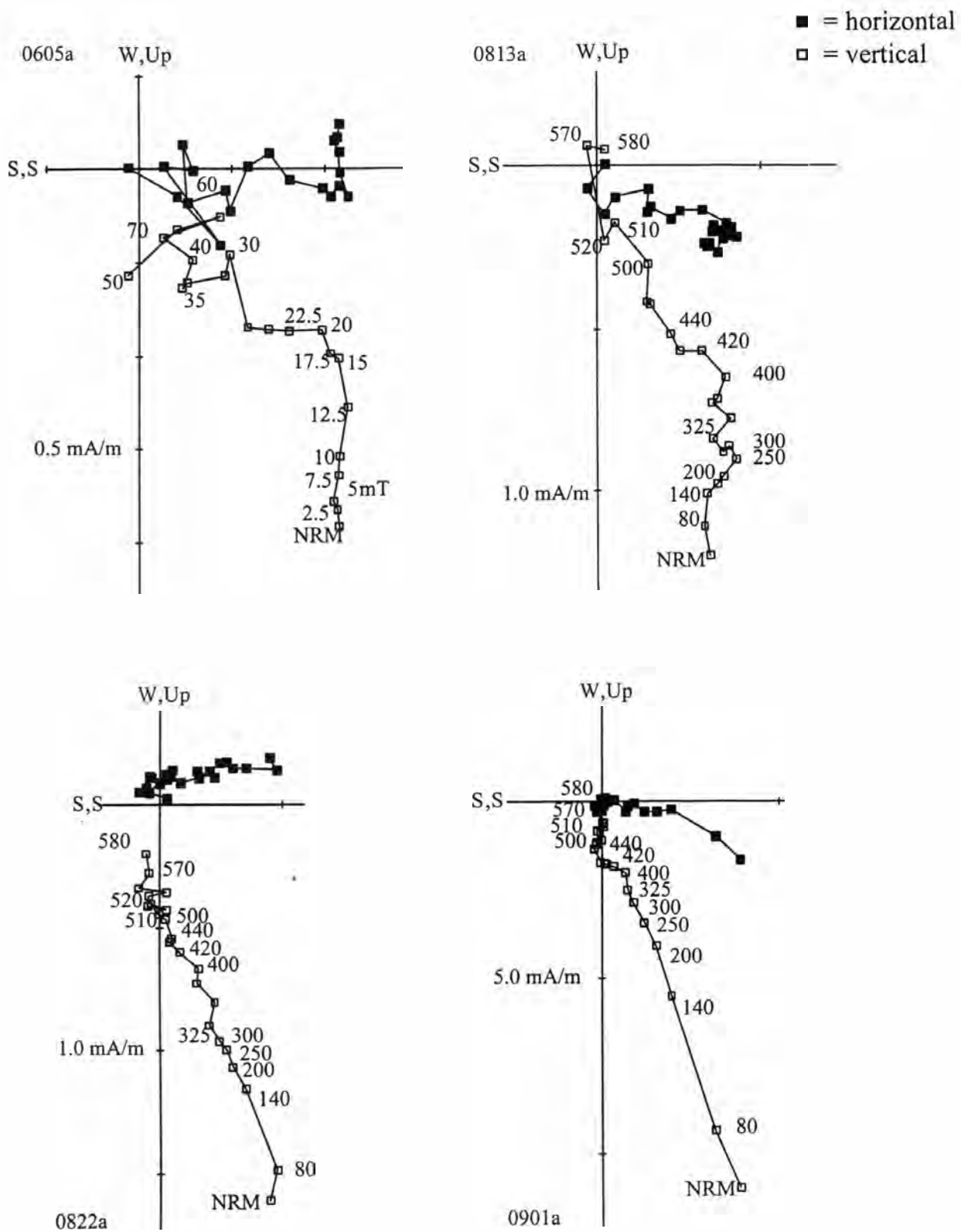


Figure 9. continued

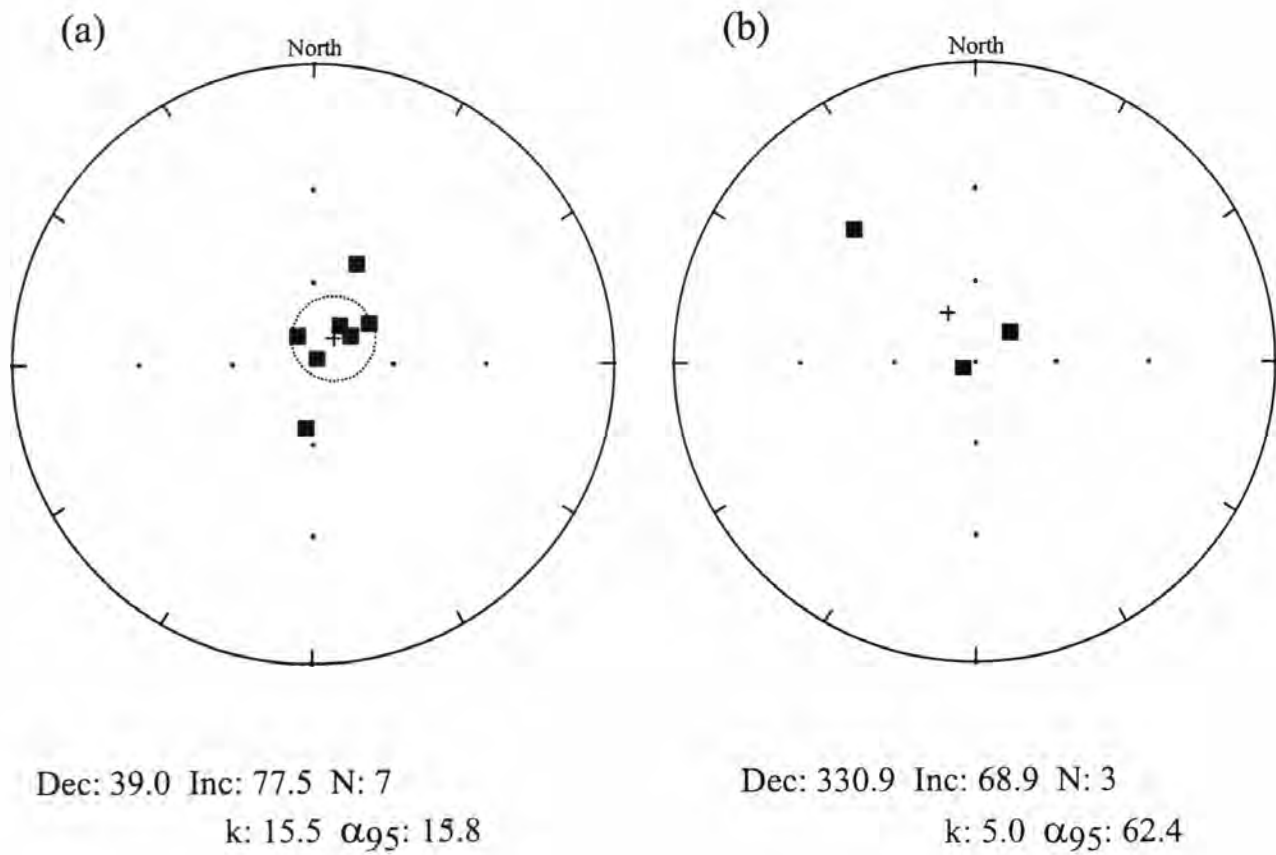


Figure 10. Equal area plots showing site-mean directions for (a) first-removed and (b) second-removed directions for the Spieden Bluff Formation.

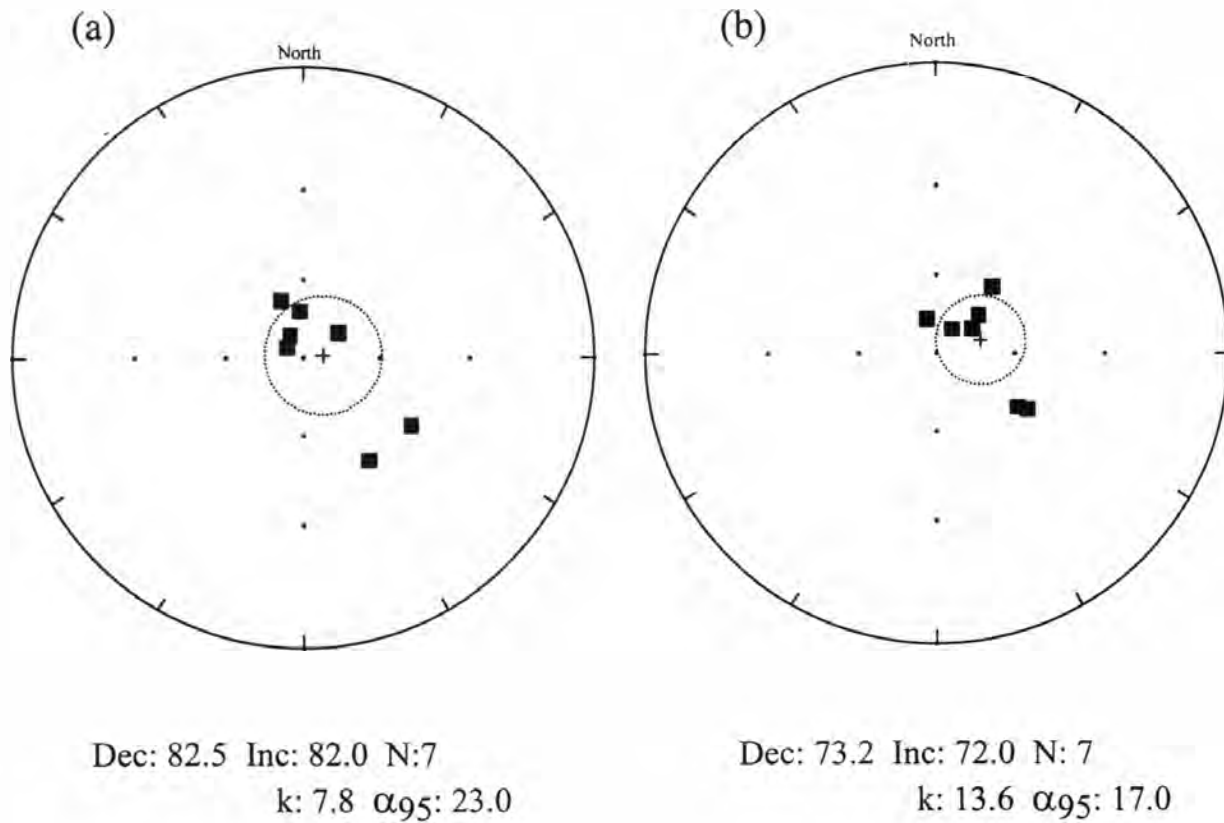


Figure 11. Equal area plots showing mean-directions in in-situ and tilt-corrected coordinates for the Jurassic Spieden Bluff Formation. (a) In-situ third-removed component (MAD < 20), (b) Tilt-corrected third-removed component (MAD < 20).



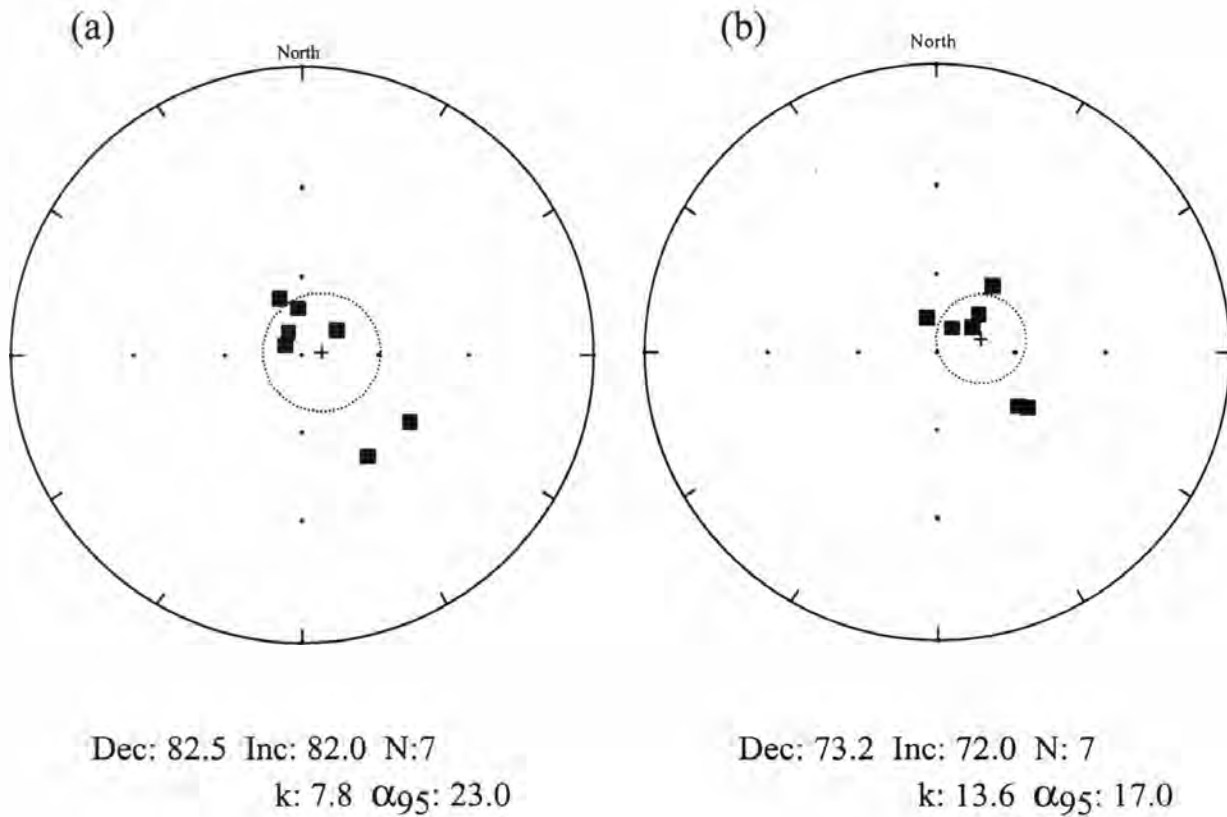


Figure 12. Equal area plots showing mean-directions in in-situ and tilt-corrected coordinates for the Jurassic Spieden Bluff Formation. (a) In-situ third-removed component (MAD < 20), (b) Tilt-corrected third-removed component (MAD < 20).

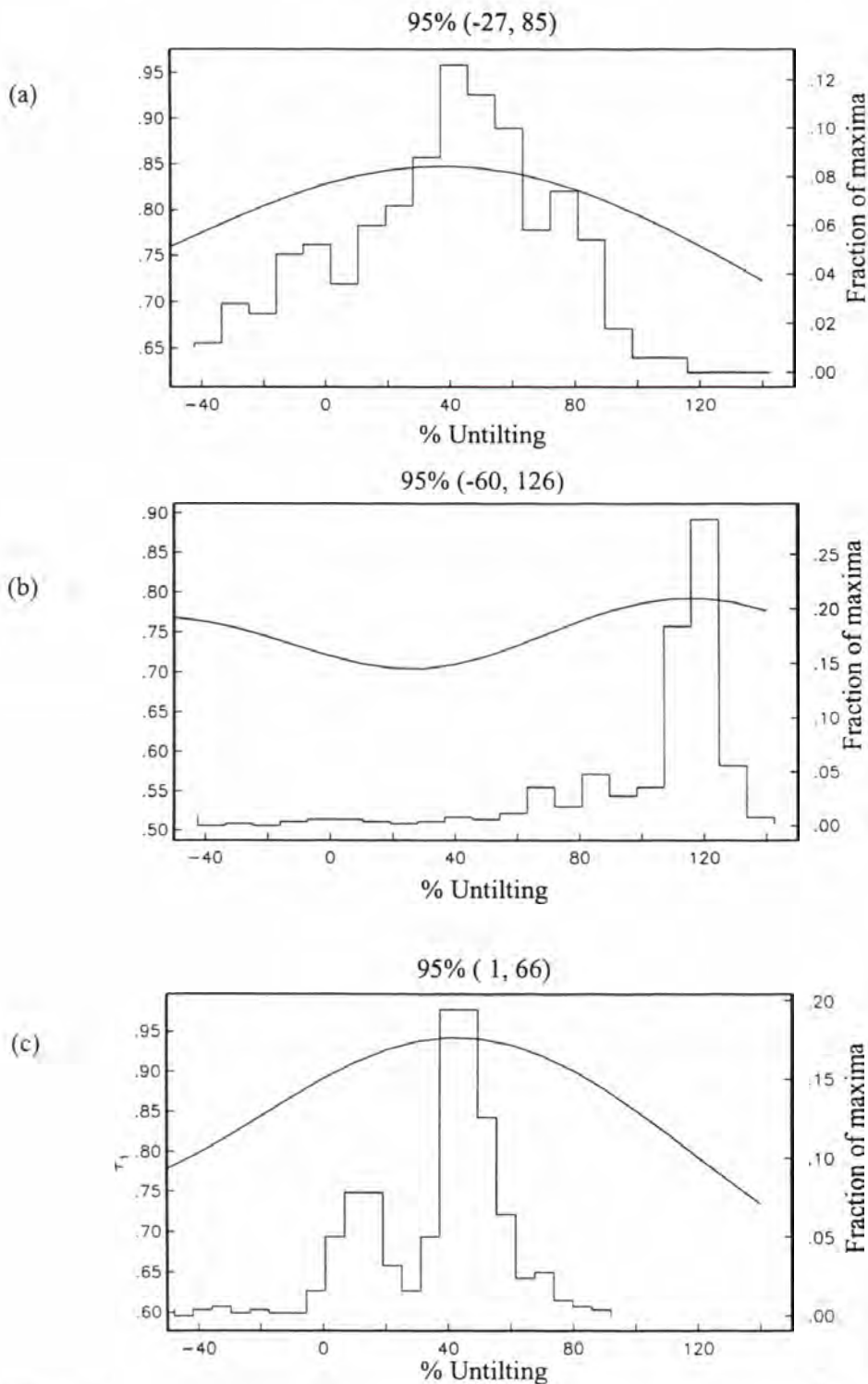


Figure 13. Incremental unfolding of the Jurassic Spieden Bluff Formation using intensity-based characteristic components. This process was performed by grouping components by the ratio of intensity of the component removed to the total intensity. Constraints required for the 95% confidence interval are located above each plot. Components with line segments of (a) ChRM60 (60-70%), (b) ChRM70 (70-80%) and (c) ChRM80 (80-90%) of the total intensity. Bootstrap method of Tauxe and Watson (1994).

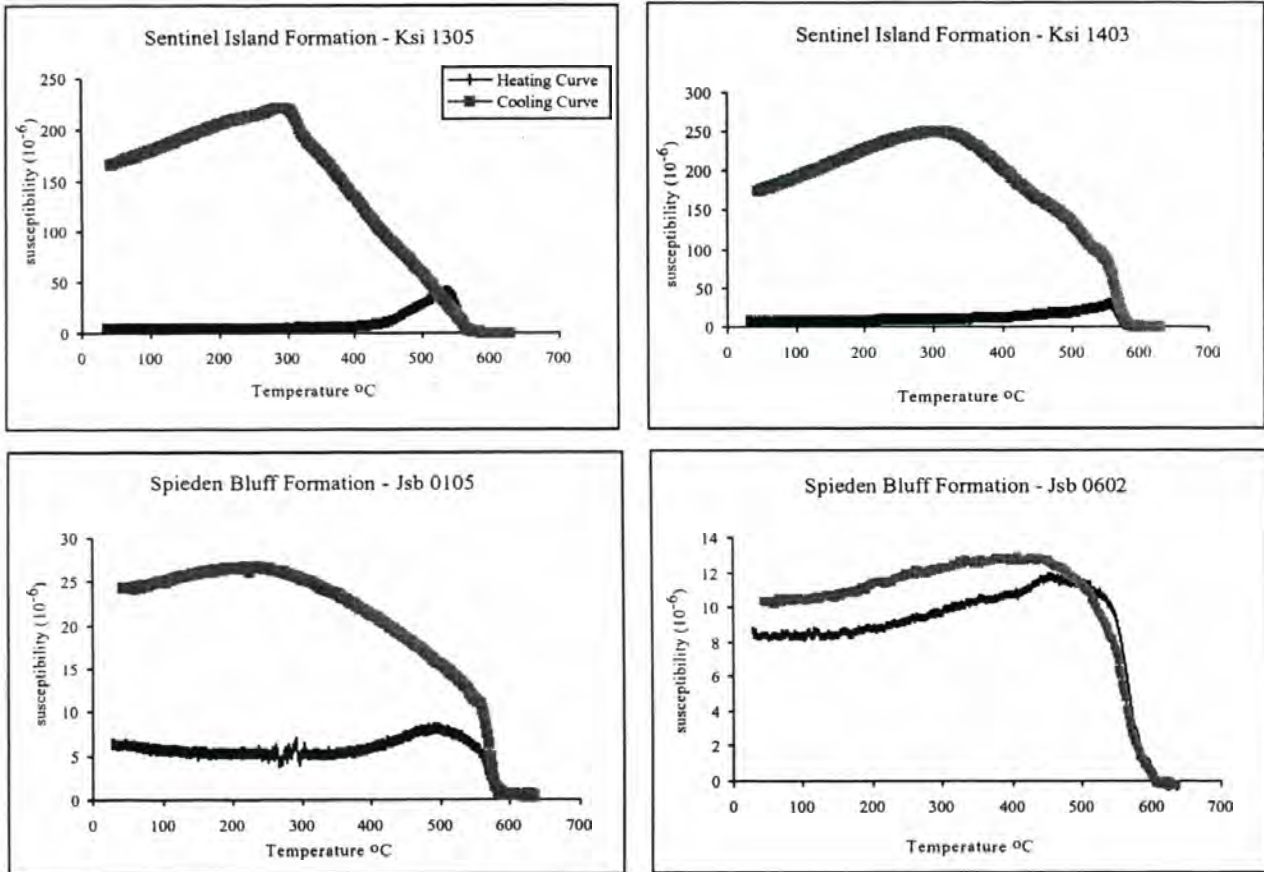


Figure 14. Plots of magnetic susceptibility against temperature for representative specimens from the Sentinel Island and Spieden Bluff formations that show the Curie temperature of magnetite (580  $^{\circ}\text{C}$ ).

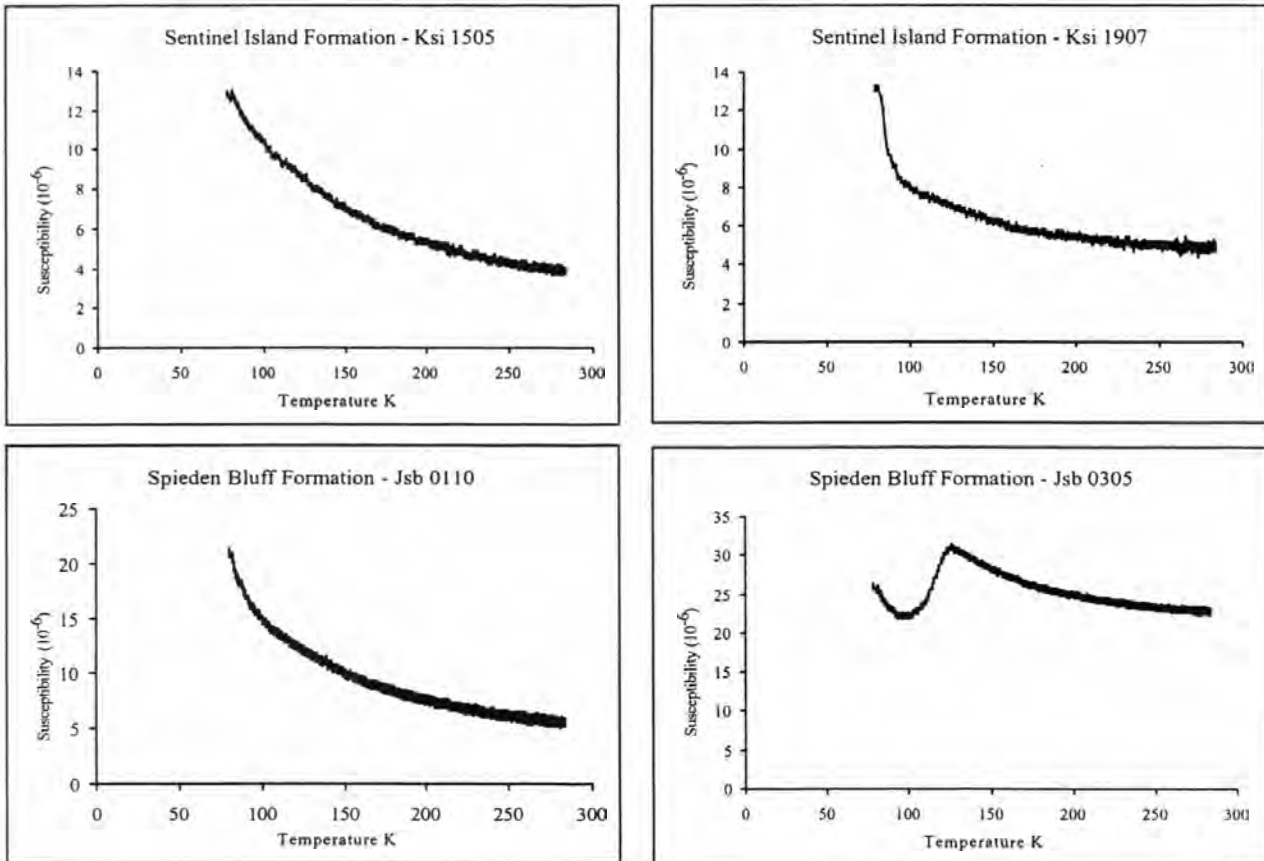


Figure 15. Representative low temperature susceptibility measurements for the Sentinel Island and Spieden Bluff formations indicating that susceptibility is dominated by paramagnetic minerals.

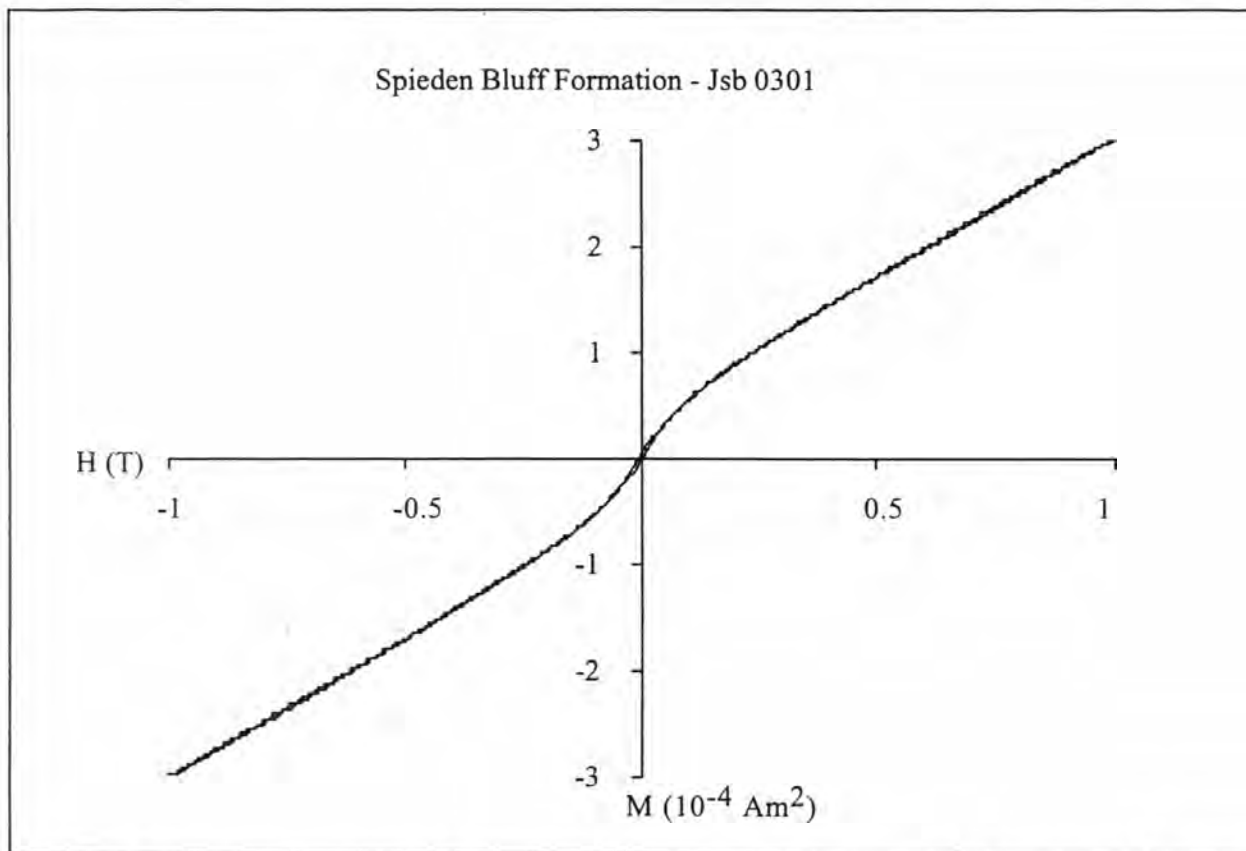
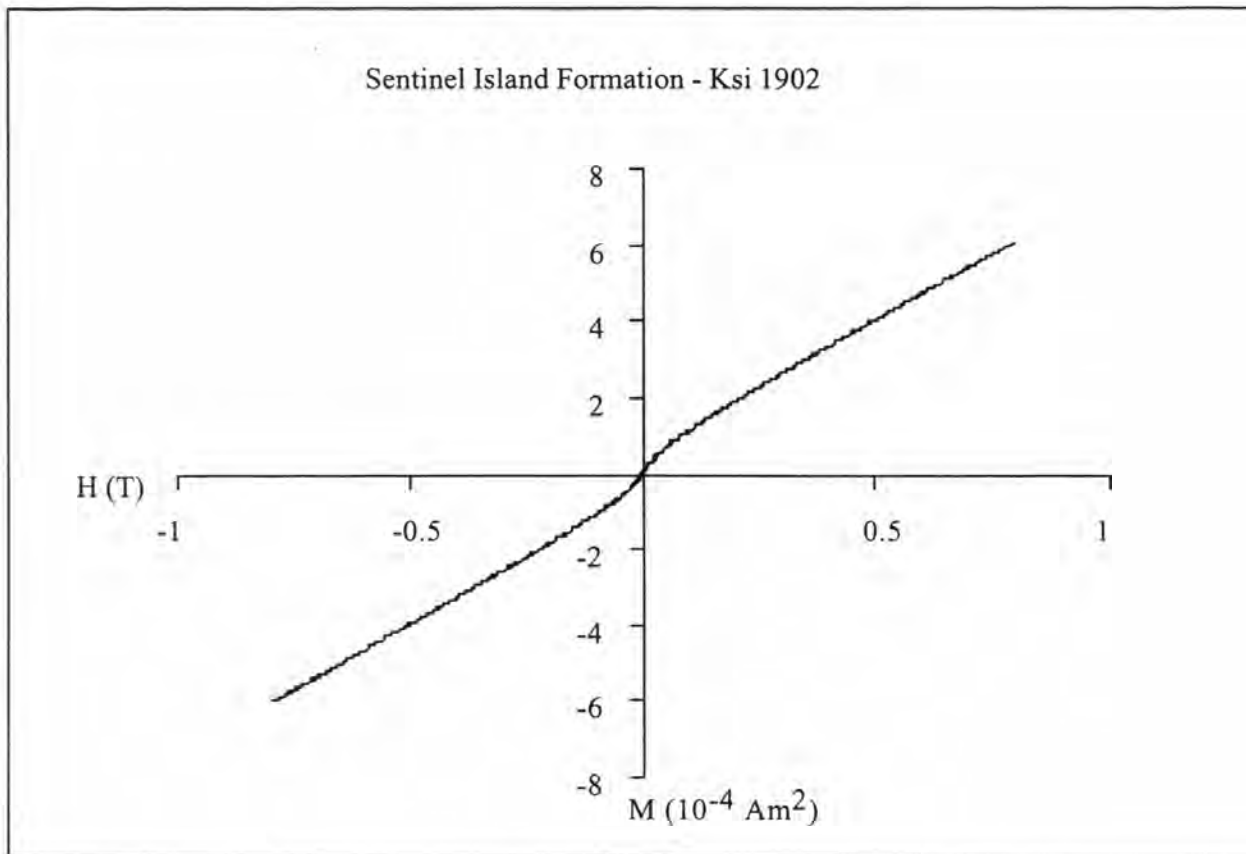


Figure 16. Representative hysteresis loops for the Sentinel Island and Spieden Bluff formations showing normal loops (non wasp-waisted loops).



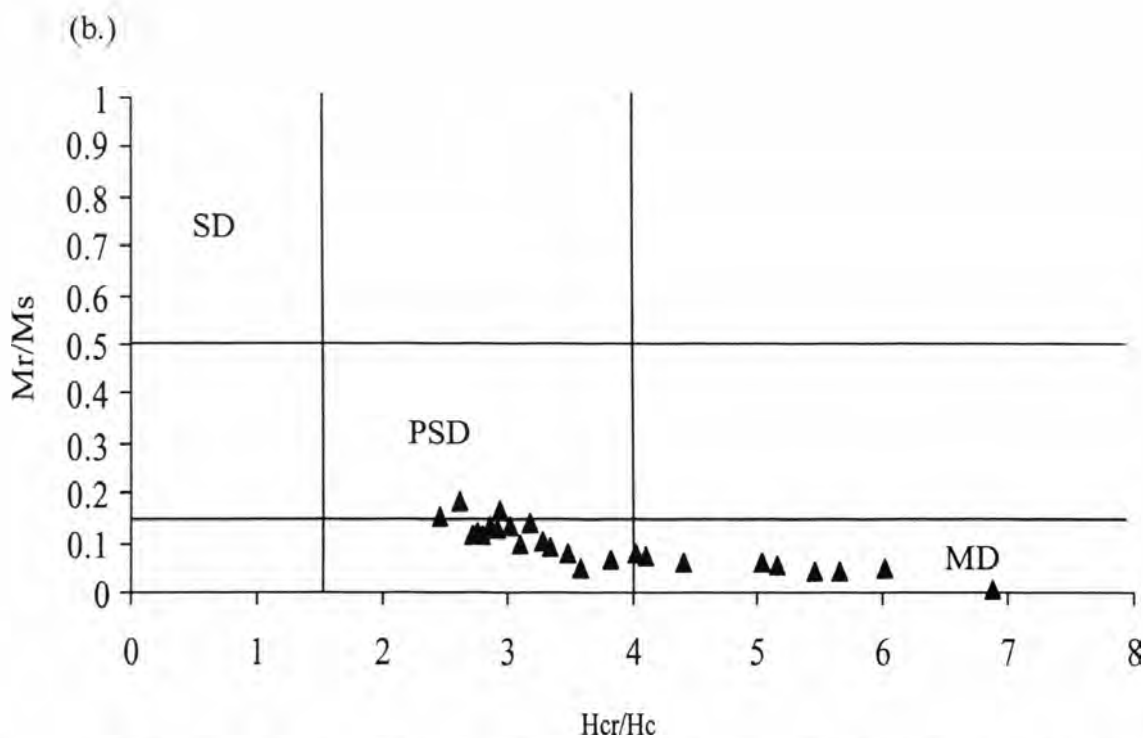
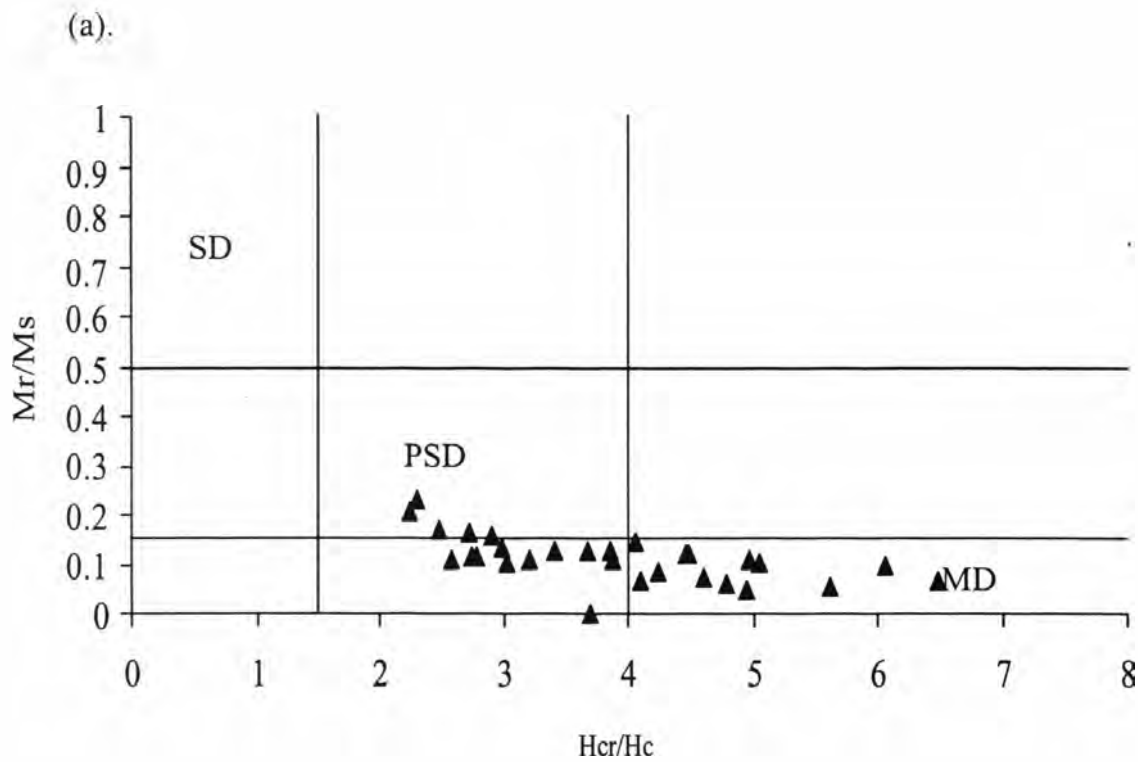


Figure 17. Day et al. (1977) plots for the (a) Sentinel Island and (b) Spieden Bluff formations indicating lack of single-domain (SD) magnetite and the presence of pseudo-single domain (PSD) and multi-domain (MD) magnetite.

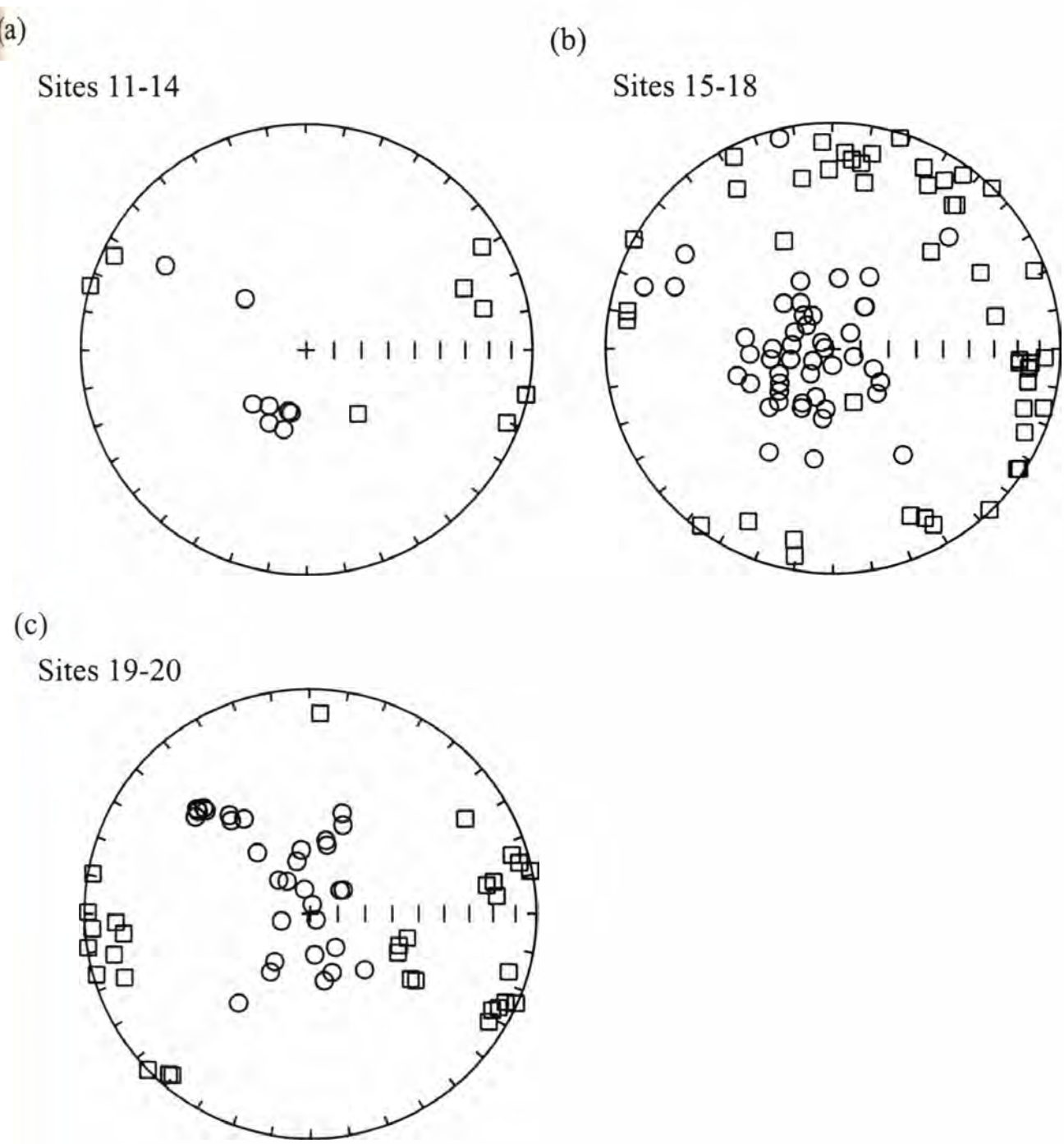
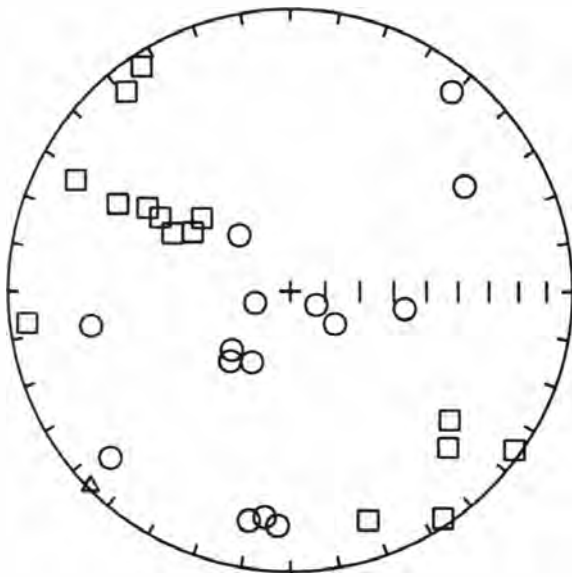
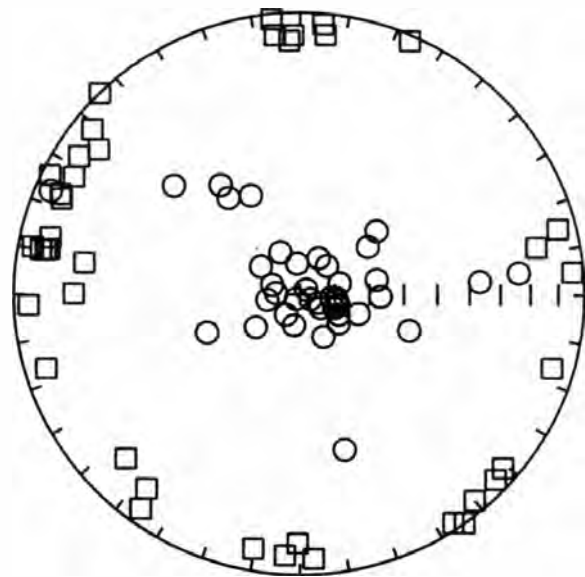


Figure 18. Anisotropy of magnetic susceptibility (AMS) for the (a-c) Sentinel Island and (d-f) Spieden Bluff Formations. Circles denote the minimum susceptibility axes and squares denote the maximum susceptibility axes. AMS axes have been tilt-corrected, so that the bedding planes are horizontal in these plots.

(d)  
Sites 1-3



(e)  
Sites 4-7

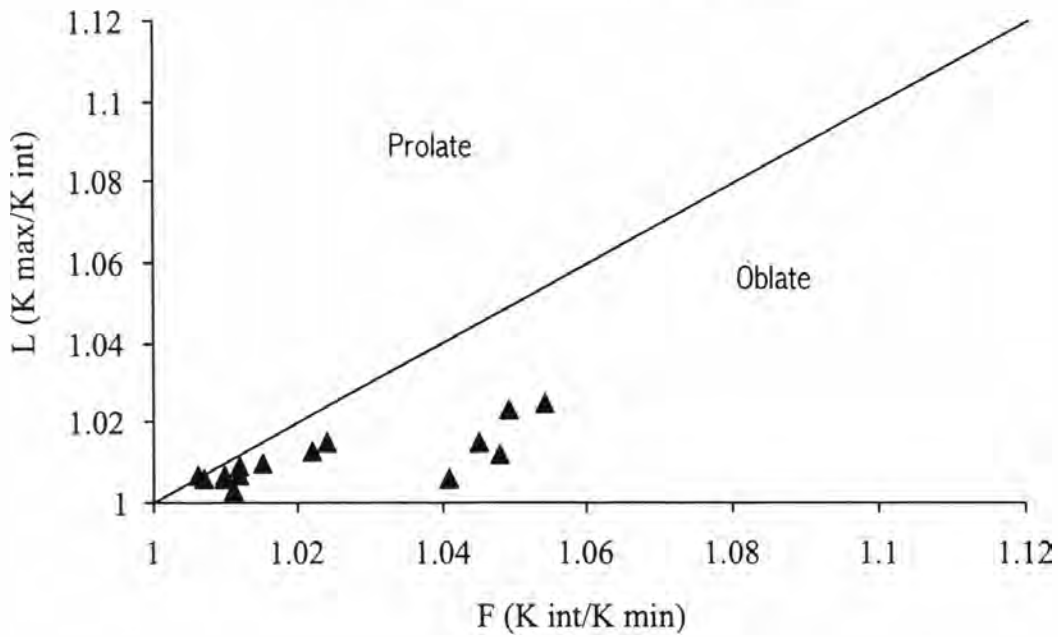


(f)  
Sites 8-9



Figure 18. continued

Sentinel Island Formation - Site Ksi 19



Spieden Bluff Formation - Site Js8 08

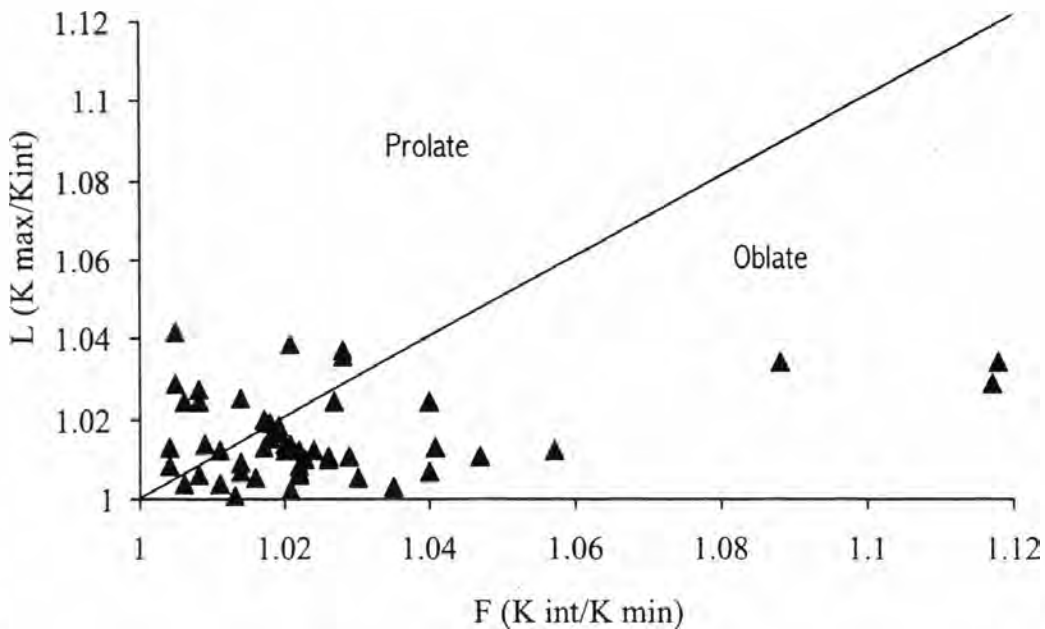


Figure 19. Flinn diagrams for the Sentinel Island and Spieden Bluff formations indicating predominant oblate anisotropy of magnetic susceptibility (AMS) fabrics.

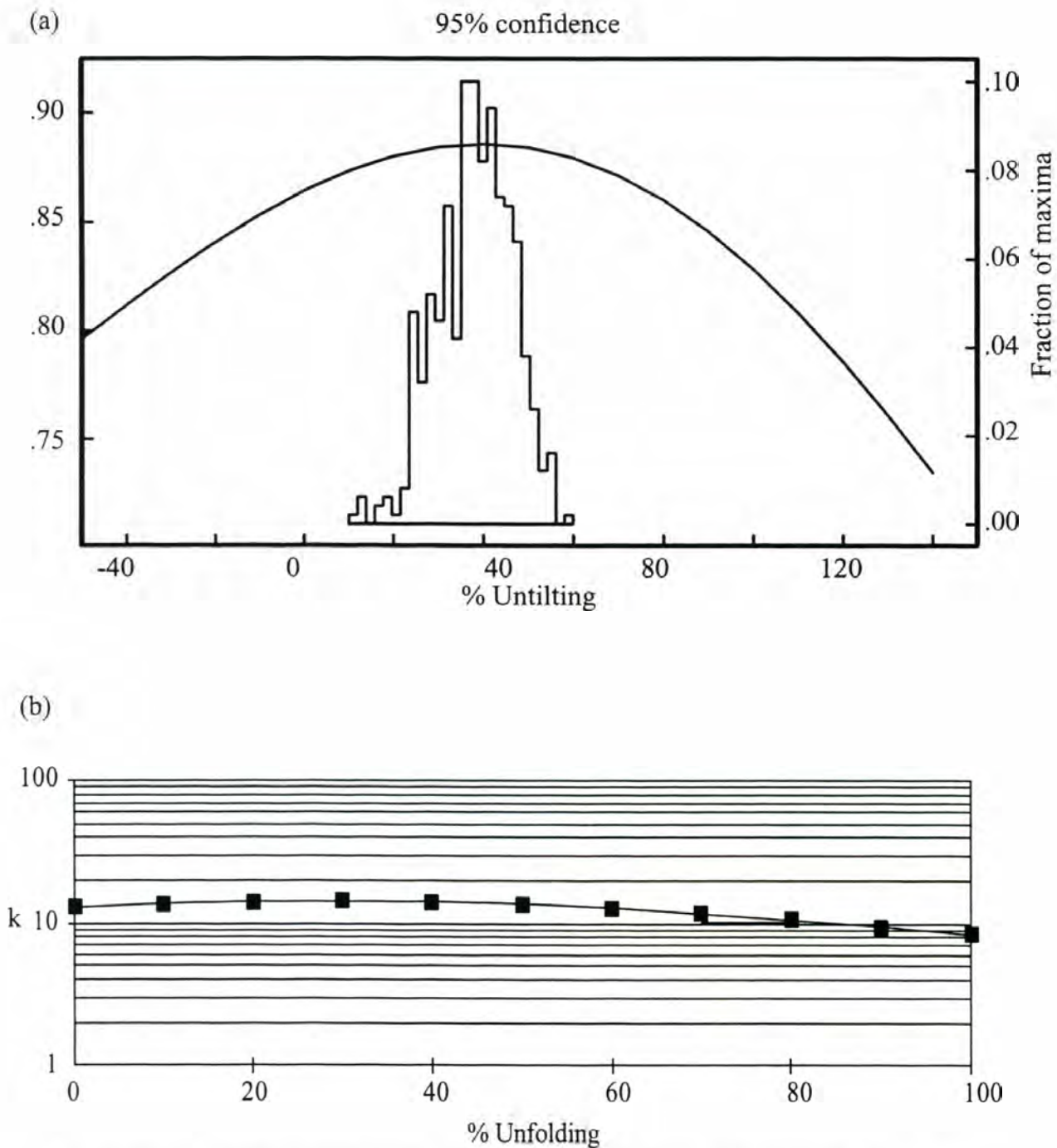


Figure 20. Fold tests show that for the Cretaceous Sentinel Island Formation directions cluster most tightly with only partial correction to horizontal, (a) after 20%-60% correction using a bootstrap method in which the histogram shows the frequency of maximum clustering for each of 1000 paradata sets (Tauxe and Watson, 1995) or (b) about 30% correction when looking for maximum in the precision parameter  $k$  (McElhinney, 1964).



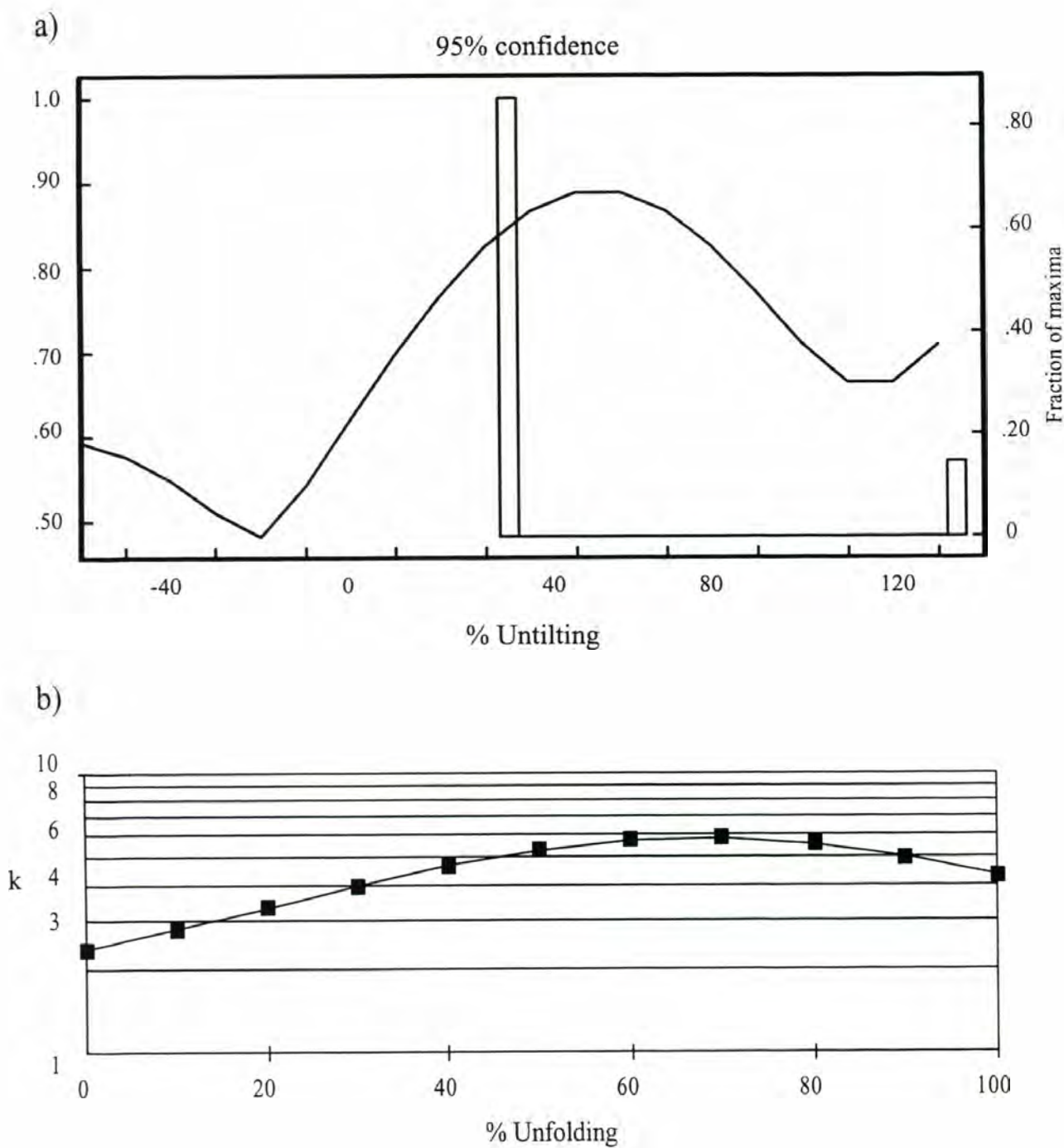
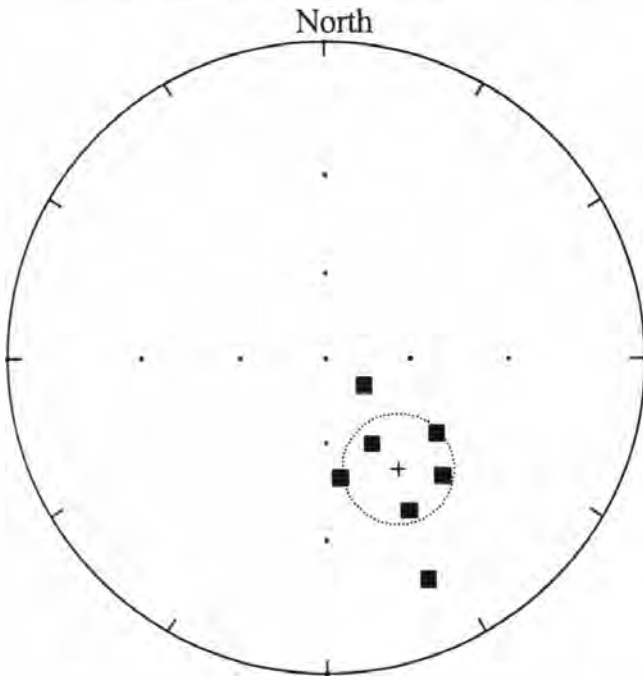


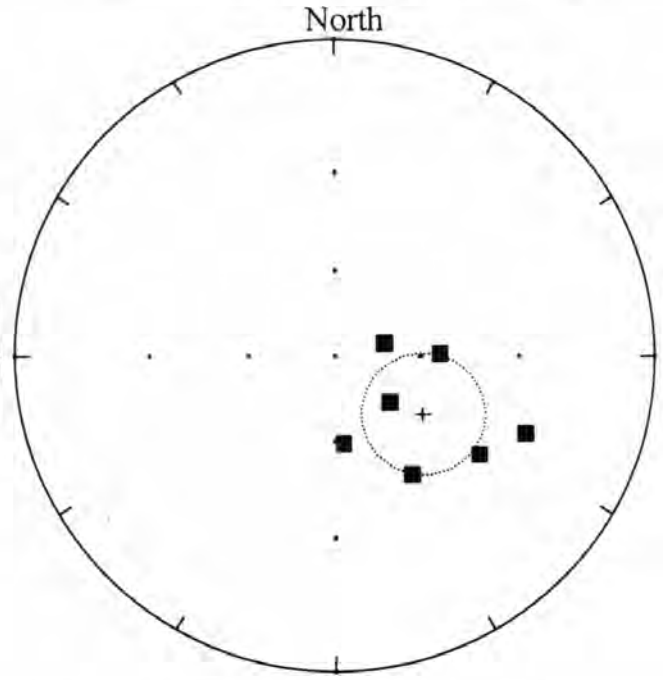
Figure 21. Fold tests of site 6 of the Jurassic Spieden Bluff Formation by (a) Tauxe and Watson (1995), and (b) McElhinney (1964) methods. Although a peak in clustering at about 70% unfolding is apparent in both tests, it is not statistically significant.

In-situ mean Site 1 (MAD < 20)



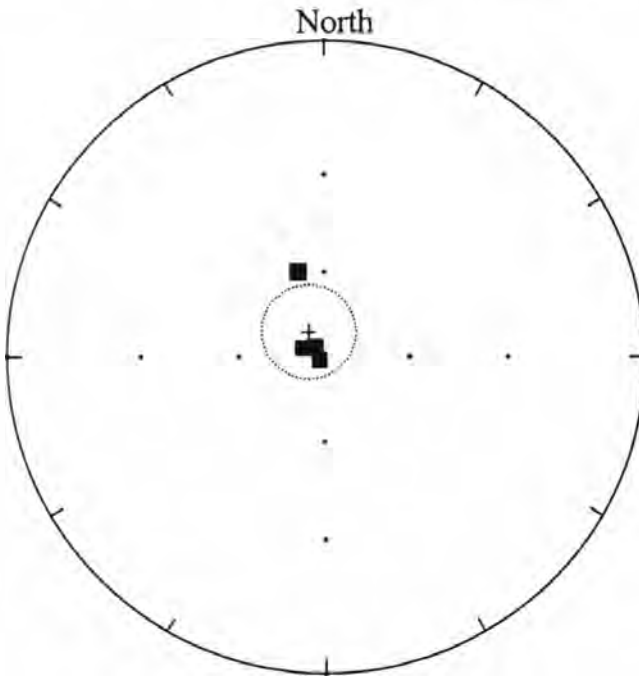
Dec: 147.0 Inc: 44.6 N: 7 k: 13.57  $\alpha_{95}$ : 17.0

Tilt Corrected Site 1 (MAD < 20)



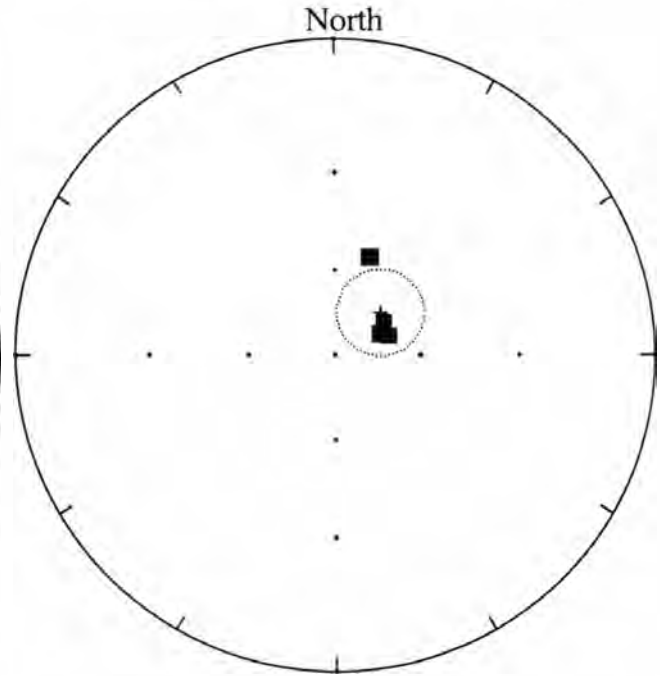
Dec: 123.6 Inc: 53.3 N: 7 k: 10.4  $\alpha_{95}$ : 19.6

In-situ mean Site 3 (MAD < 20)



Dec: 328.6 Inc: 79.5 N: 4 k: 30.70  $\alpha_{95}$ : 16.8

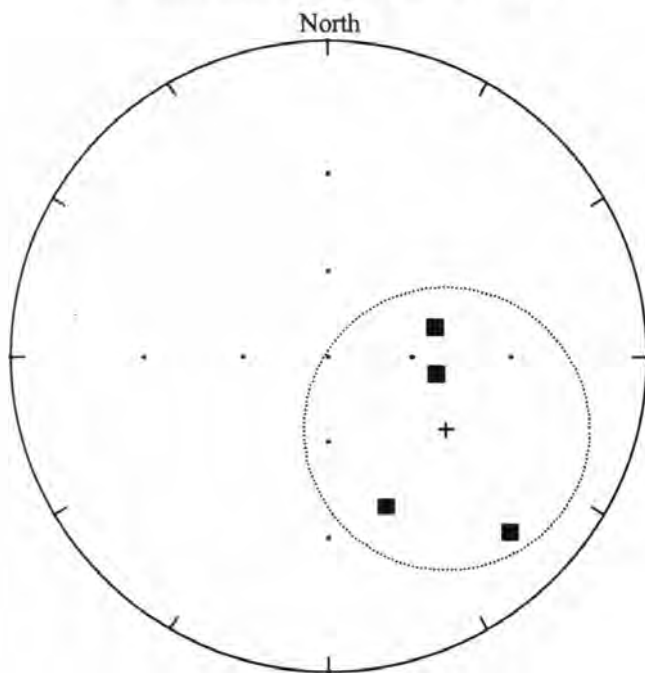
Tilt Corrected Site 3 (MAD < 20)



Dec: 47.0 Inc: 67.8 N: 4 k: 38.15  $\alpha_{95}$ : 15.1

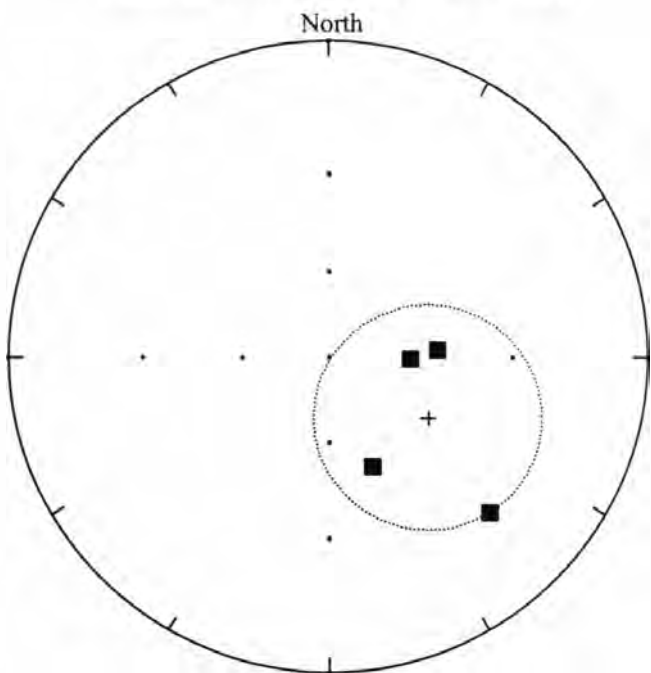
Figure 22. Equal area diagrams showing site level in-situ and tilt-corrected directions for the Spieden Bluff Formation.

In-situ mean Site 4 (MAD < 20)



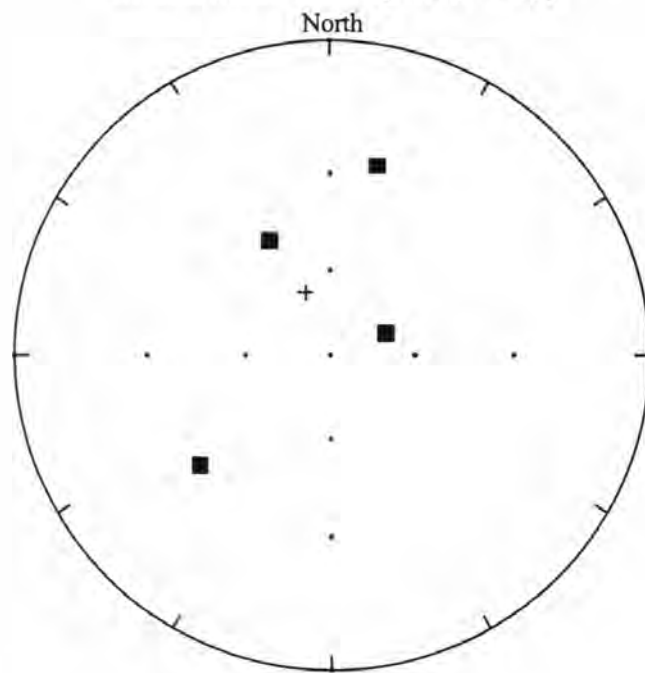
Dec: 121.7 Inc: 42.7 N: 4 k: 6.16  $\alpha_{95}$ : 40.3

Tilt Corrected Site 4 (MAD < 20)



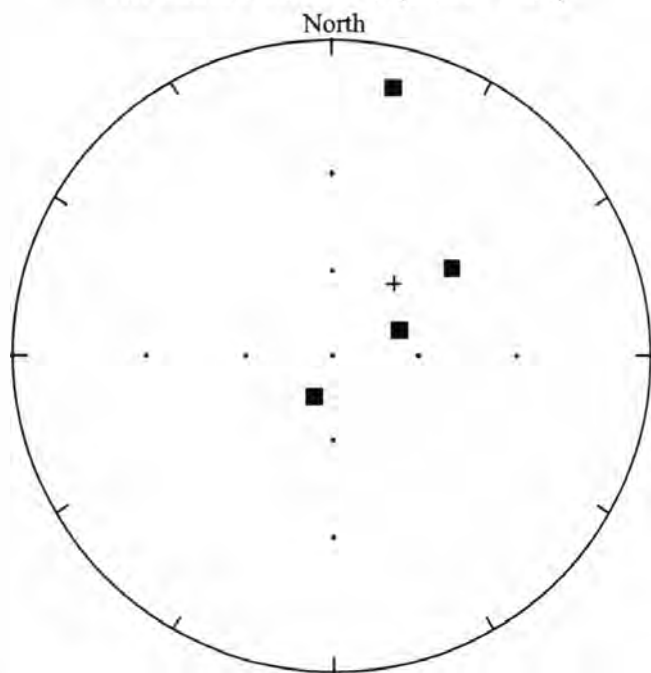
Dec: 121.7 Inc: 50.0 N: 4 k: 8.01  $\alpha_{95}$ : 34.6

In-situ mean Site 6 (MAD < 20)



Dec: 338.7 Inc: 65.9 N: 4 k: 2.68  $\alpha_{95}$ : 70.6

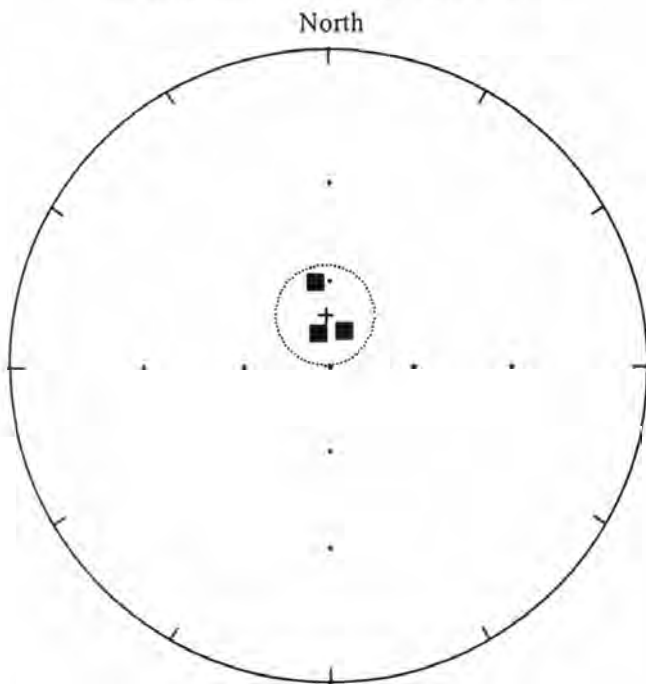
Tilt Corrected Site 6 (MAD < 20)



Dec: 39.8 Inc: 56.8 N: 4 k: 3.59  $\alpha_{95}$ : 56.8

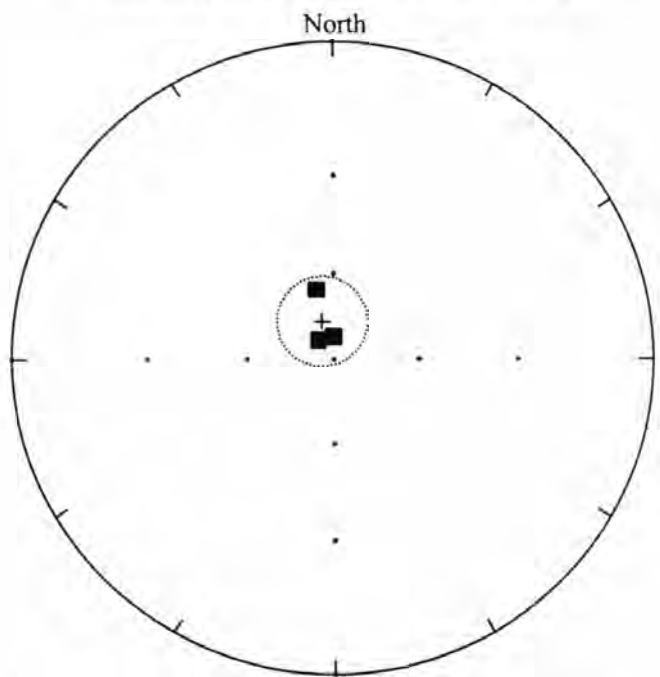
Figure 22. continued.

In-situ mean Site 7 (MAD < 20)



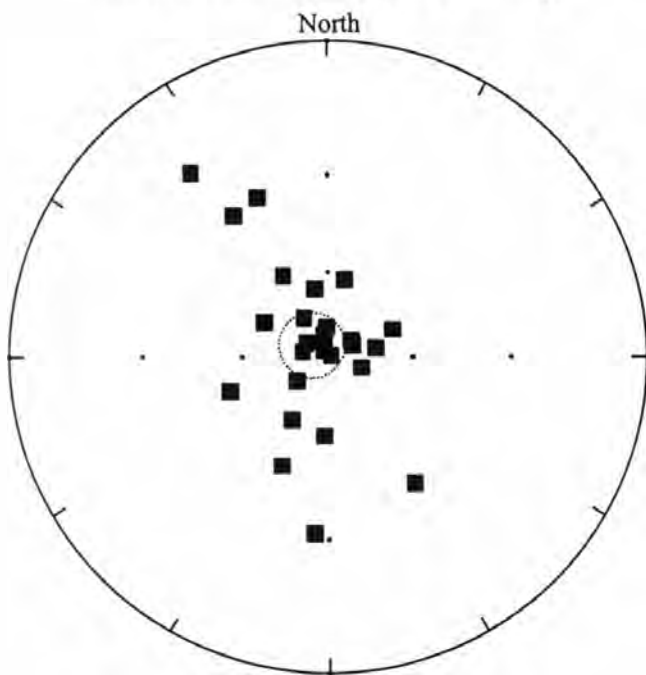
Dec: 355.4 Inc: 71.4 N: 3 k: 51.5  $\alpha_{95}$ : 17.4

Tilt Corrected Site 7 (MAD < 20)



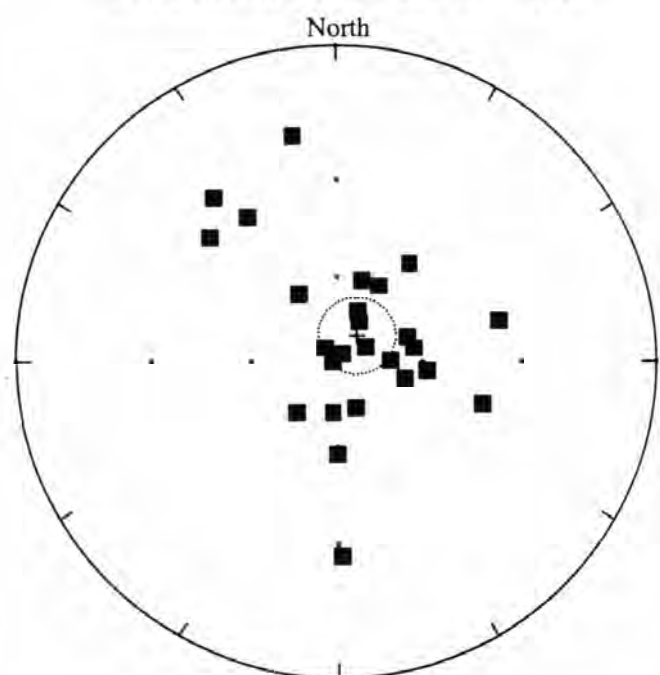
Dec: 343.8 Inc: 75.8 N: 3 k: 62.46  $\alpha_{95}$ : 15.7

In-situ mean Site 8 (MAD < 20)



Dec: 306.8 Inc: 82.9 N: 26 k: 6.67  $\alpha_{95}$ : 11.9

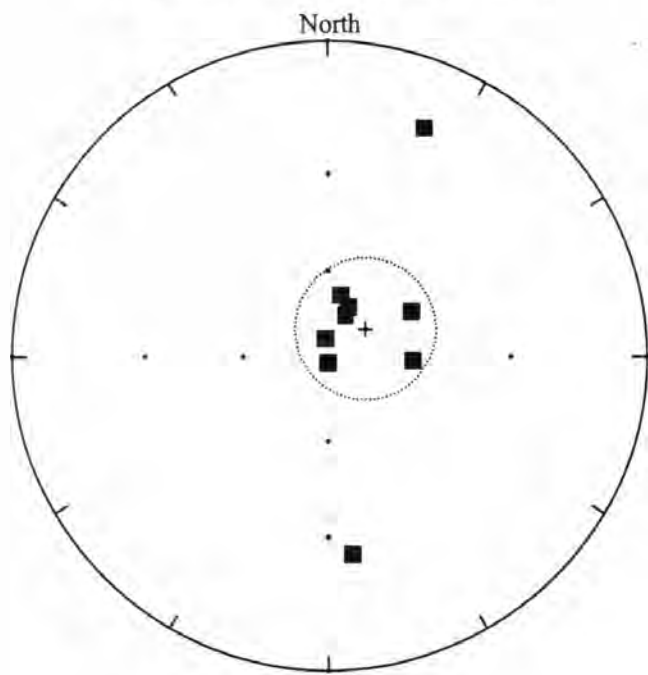
Tilt Corrected Site 8 (MAD < 20)



Dec: 37.7 Inc: 78.3 N: 26 k: 5.29  $\alpha_{95}$ : 13.7

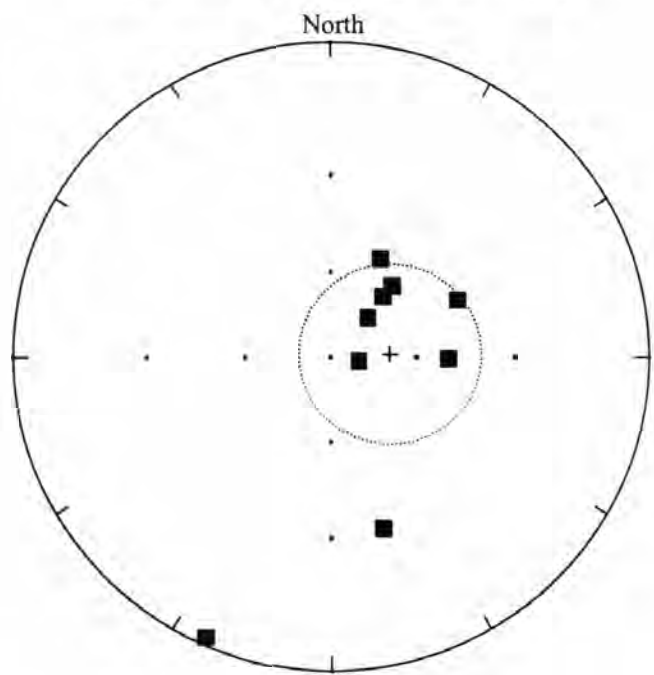
Figure 22. continued.

In-situ mean Site 9 (MAD < 20)



Dec: 54.1 Inc: 73.2 N: 9 k: 5.33  $\alpha_{95}$ : 24.6

Tilt Corrected Site 9 (MAD < 20)



Dec: 87.3 Inc: 68.9 N: 9 k: 3.78  $\alpha_{95}$ : 30.7

Figure 22. continued.

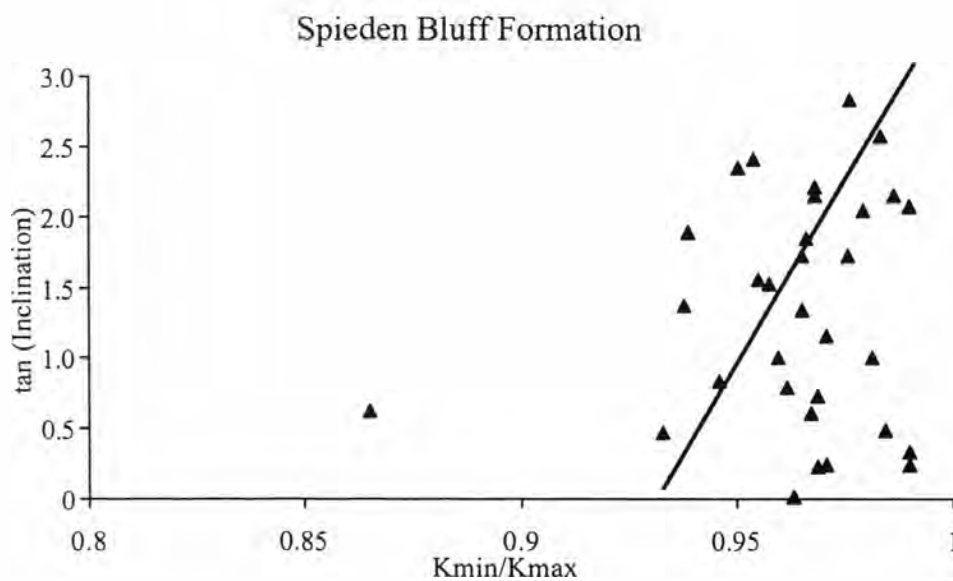
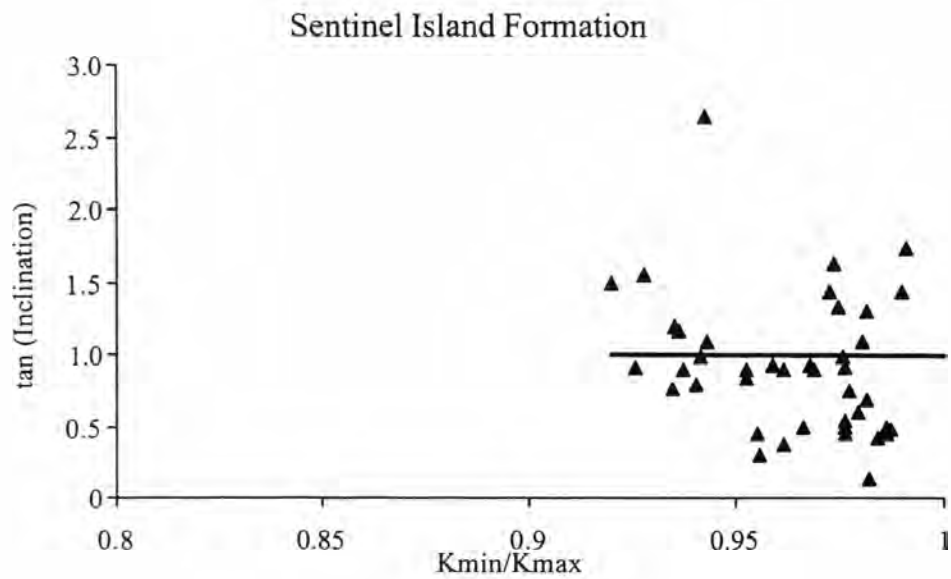


Figure 23. Magnetic susceptibility of anisotropy (AMS), plotted as  $K_{min}/K_{max}$  ( $1/P$ ) (degree of anisotropy) versus tangent of inclination (after Hodych et al., 1999) for the Sentinel Island and Spieden Bluff Formations. These plots show no clear relationship between shallow inclinations and more-anisotropic AMS fabrics, as would be expected for significant inclination-shallowing.



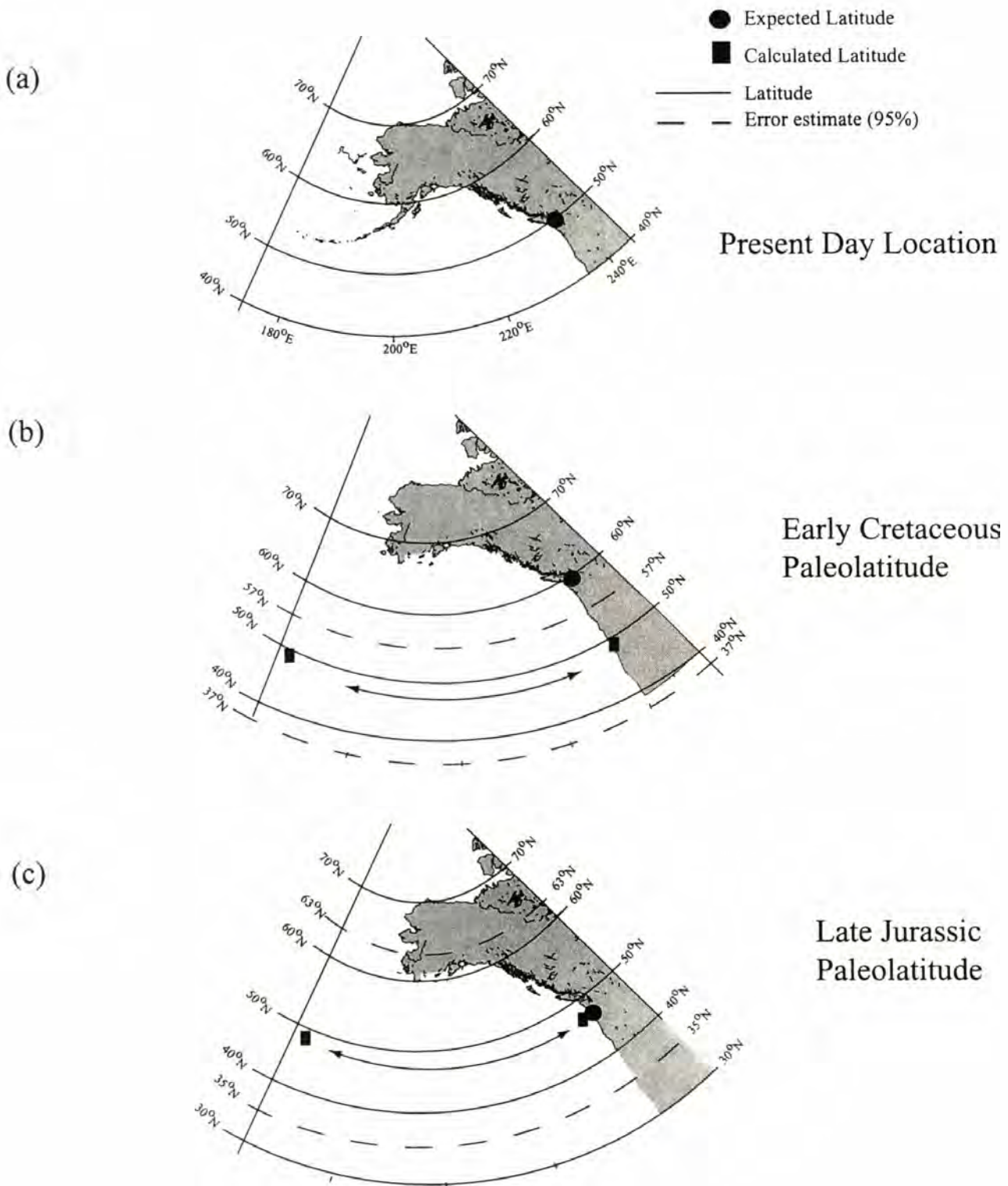


Figure 24. Reconstruction maps for the paleolatitudes of the Spieden Group. Present day latitude  $48.6^{\circ}$  N of the Spieden Group is indicated (a), and paleolatitudes based on this study for (b) Cretaceous Sentinel Island Formation, latitude  $45.7^{\circ}$  N, and (c) Jurassic Spieden Bluff Formation, latitude  $47^{\circ}$  N. Paleolatitudes for North America are determined from these reference poles: (b) Early Cretaceous, Cretaceous Still Stand Pole ( $71.4^{\circ}$  N,  $195.9^{\circ}$  E) (McEnroe, 1996, Van Fossen and Kent, 1992), and (c) Late Jurassic, Brushy Basin Member of the Morrison Formation ( $68.3^{\circ}$  N,  $156.2^{\circ}$  E) (Bazard and Butler, 1994).